WINDOWS INTO SAUROPSID AND SYNAPSID EVOLUTION
Essays in honor of Prof. Louis L. Jacobs, pp. 66–98, 2023

REMARKABLY WELL-PRESERVED *IN-SITU* GUT-CONTENT IN A SPECIMEN OF *PROGNATHODON KIANDA* (SQUAMATA: MOSASAURIDAE) REVEALS MULTISPECIES INTRAFAMILIAL PREDATION, CANNIBALISM, AND A NEW MOSASAURINE TAXON

Michael J. Polcyn[1,3,*], Anne S. Schulp[2,3], and António Olímpio Gonçalves[4]

[1]Roy M. Huffington Department of Earth Sciences, Southern Methodist University, Dallas, Texas, USA, mpolcyn@smu.edu
[2]Naturalis Biodiversity Center, Leiden, The Netherlands
[3]Utrecht University, Utrecht, The Netherlands
[4]Departamento de Geologia, Faculdade de Ciências, Universidade Agostinho Neto, Luanda, Angola

ABSTRACT In this contribution we report a spectacularly well-preserved, semi-articulated specimen of *Prognathodon kianda* containing three partial mosasaurs in its stomach region. The discovery is from the lower Maastrichtian (~71.5Ma) "Bench 19 Bonebed" at Bentiaba, Angola. Each of the three mosasaurs found in the gut region is a unique taxon, one being the first documented occurrence of cannibalism in mosasaurs, and another representing a new mosasaurine genus and species, *Bentiabasaurus jacobsi* gen. et sp. nov., a taxon closely related to *Mosasaurus*. Trophic interactions at the "Bench 19 Bonebed" locality appear to be controlled in part by relative size of the predator and the prey, all prey taxa falling between 43 and 57% of the predator's body length. Prey items are all dismembered to some degree and individual parcels approach the estimated maximum sizes that can pass the gullet. Tooth and bone modification, and other aspects of prey processing are discussed. Though the sample is small, the observed range of modalities suggests prey processing, digestive biology, and methods of elimination in mosasaurs was diverse.

KEYWORDS Predator, Prey, Mosasaurid, Gut-content, Regurgitaliths, Cannibalism, Feeding ecology

INTRODUCTION

Mosasaurs are marine-adapted lizards that occupied the top predator niche in many marine ecosystems towards the end of the late Cretaceous. There are numerous reports of mosasaur predation on invertebrates such as cephalopods, pteriomorphian bivalves, and echinoderms (e.g., Dollo, 1913; Kauffman, 2004; Martin and Fox, 2007; Konishi et al., 2011; Neumann and Hampe, 2018), and also of predation and consumption of vertebrates, including fishes, plesiosaurs, turtles, and birds (e.g., Dollo, 1887; Williston, 1899; Sternberg, 1922; Camp, 1942; Martin and Bjork, 1987; Everhart, 2004a; Einarsson et al., 2010; Konishi et al, 2011, 2014). However, there are few reports of mosasaur-on-mosasaur predation. Furthermore, evidence of trophic interactions between mosasaurs is relatively rare and mostly in the form of trauma inflicted by other mosasaurs (Everhart, 2008; Bastiaans et al., 2020; Tykoski and Polcyn, 2023).

Longrich et al. (2022) recently presented a number of mosasaurid specimens displaying varying degrees of erosion and decalcification of teeth and bones, which they interpreted as disgorged stomach content, hypothesizing these were in fact mosasaur gastric pellets, or regurgitaliths (see also Cooper et al., 2022). Furthermore, Longrich et al. (2022) argued the maker of the pellets was likely *Thalassotitan atrox,* a gigantic predatory mosasaurid nested among *Prognathodon* in their phylogenetic analysis. Additionally, Martin and Bjork (1987) interpreted large masses of commutated fish material, in one case containing ammonite "hash", and in another putative plesiosaur gastroliths, as possibly representing mosasaur coprolites, though qualifying their interpretations as "somewhat conjectural". In light of the interpretations of Longrich et al. (2022), the coprolites reported by Martin and Bjork (1987) may also represent regurgitaliths.

Direct evidence of mosasaur-on-mosasaur predation, in the form of *in-situ* gastric content, is exceedingly rare. Russell

*Corresponding author

(1967, p. 69) citing Anonymous (1962, p. 5), briefly mentioned "possible cannibalism reported from Canada where fragments of a small mosasaur were found mixed with the skeleton of a larger one", but that occurrence has not been described. There are two reports of predation of mosasaurs by the mosasaur genus *Tylosaurus* (Martin and Bjork, 1987; Bell and Barnes, 2007). The gut-content reported by Martin and Bjork (1987) contained a mix of taxa, including parts of the mosasaur *Latoplatecarpus* sp., fishes, and the sea bird *Hesperornis* sp., consumed by a *Tylosaurus proriger*. In a conference abstract, Bell and Barnes (2007) reported portions of the mosasaur *Plesioplatecarpus planifrons* and the durophagous shark *Ptychodus mortoni* in the gut region of a specimen of *Tylosaurus nepaeolicus*. Strganac et al. (2015a) briefly reported two occurrences of mosasaur stomach content, one in the gut region of a specimen of *Prognathodon kianda* (Fig. 1), and the other as an isolated multi-taxon mass of partially decalcified bones, interpreted as disgorged stomach content. Since that report, one of those specimens has been prepared for study and is the subject of this contribution.

The occurrences briefly reported by Strganac et al. (2015a) come from the Lower Maastrichtian (~71.5 Ma) locality of Bentiaba, Namibe Province, Angola, which was located at approximately 24°S paleolatitude (Jacobs et al., in press) at that time, placing it in a highly productive upwelling zone, analogous to that seen along the west coast of Africa between 15° and 30°S latitude today, an area known as one of the world's most productive fisheries. The sediments at the locality were deposited relatively nearshore on a narrow continental shelf, in waters approximately 50-100 meters deep, and a water temperature of ~18°C (Strganac et al., 2015b). All of these are contributing factors to the high concentration of vertebrate fossils found at the locality today, which has produced a large number of marine amniote specimens, including mosasaurs (Schulp et al., 2008; Schulp et al, 2013; Polcyn et al., 2010), plesiosaurs (Araújo et al., 2015a; 2015b; Marx et al., 2022), and marine turtles (Mateus et al, 2012). Many of the fossils collected at Bentiaba show evidence of scavenging in the form of tooth marks on various elements of mosasaur, plesiosaur, and turtle carcasses left by the teeth of the anacoracid shark *Squalicorax pristodontus* and to a lesser extent, *Cretalamna* sp. (Fig. 2; see also Strganac et al., 2015a).

We report here a remarkable example of well-preserved, in-situ mosasaur gut-content, containing three partial mosasaurs, each a unique taxon, one being the first documented instance of cannibalism in mosasaurs, and another representing a new genus and species closely related to *Mosasaurus*. We first provide a brief overview of the gut-content association, then address each of the prey taxa systematically, including the naming, describing, and diagnosing the new mosasaurine taxon, and close with a discussion of feeding and digestive biology of mosasaurs.

METHODS

Specimen preparation — The specimen MGUAN PA183 (and associated materials) was excavated with power and hand tools, and removed in seven plaster jackets and numerous hand samples. It was prepared at SMU with air-scribes and hand tools, and bones were treated with PVA. Once taken to the preparation stage shown in Fig. 1, the specimen was molded and cast in polyurethane resin. The resin casts were scanned with an Artec Leo (Artec Inc., Luxembourg) to generate 3d surface models, which were rendered in Lightwave 3D 2020 (Lightwave Digital, Stevenage, UK) to produce Fig. 1. Subsequent to mold making, the blocks were prepared further removing bones from matrix for study.

CT scanning — CT scanning was performed at the University of Texas high-resolution X-ray computed tomography facility in Austin, Texas, USA, producing 3 scan data sets used for study and to produce Figs. 6, 7, 9, and 12. The scans were processed in Amira 6.3 (ThermoFisher Scientific, Waltham, Massachusetts, USA).

Institutional Abbreviations — **MGUAN PA**, Projecto PaleoAngola collection in the Museum of Geology, Universidade Agostinho Neto, Luanda, Angola; **MHNM**, Museum of Natural History of Marrakech at Cadi Ayyad University, Morocco; **NDGS**, North Dakota Geological Survey, Bismarck, ND, USA; **SMU**, Southern Methodist University Shuler Museum of Paleontology, Dallas, TX, USA; **YPM**, Yale Peabody Museum, New Haven, CT, USA.

RESULTS

The specimen MGUAN PA183 is a semi-articulated skeleton of an adult *Prognathodon kianda* (Schulp et al., 2008), missing most of the tail due to recent erosion, and most of the ribs, limbs, and girdles due to ancient scavenging

(Fig. 1A). The vertebral column is nearly completely articulated, with four trunk vertebrae just posterior to the cervical series, and the articulated series of the last thirteen trunk vertebrae slightly displaced. Proximal portions of ribs are found on both sides of the vertebral column in the cervical and thoracic region but more posteriorly, they appear to have been completely removed by scavengers, except for a few small fragments. The skeleton of the predator is well preserved, but postdepositional cracking and displacement is common (Fig. 2A).

Teeth and bone surfaces of the predator (MGUAN PA183) are well preserved, showing no sign of erosion; however, some skull elements and ribs preserve signs of predation by sharks, including fine parallel grooves such as those made by the serrated teeth of *Squalicorax pristodontus* (Fig. 2B-D), as well as punctures and isolated grooves, likely inflicted by *Cretalamna* sp. (Fig. 2E-G) suggesting the missing elements including the ribs, girdles, and limbs were likely removed by large scavengers such as these. Numerous remains of bony fishes of different sizes, a single sawfish rostral tooth, and shed mosasaur teeth attributable to *Prognathodon kianda*, were collected on and around the carcass in the field and during laboratory preparation of the field jackets (cataloged as MGUAN PA183A 1-n), but show no evidence of acid etching or other indication of travel through the digestive tract and are interpreted as a time-averaged sample of additional scavengers and/or background attrition. The locality is extremely fossiliferous, and thus the recovery of fishes and mosasaur remains in the sediments underlying, overlying and surrounding the carcass are expected. There are only a small number of examples of fish remains that were found in close association with the bone layer, but again, none of these are acid etched or worn in such a way as to indicate they were ingested. More likely, they were attrition of the scavenging community that developed around this carcass.

The carcass of the predator (MGUAN PA183) is lying upside down, and based on the pattern of rib preservation, its visceral cavity was apparently opened and facing up, prior to burial. Remains of three other mosasaurs are lying primarily on the left side of the carcass, roughly parallel to the vertebral column (Fig. 1A and B), spanning trunk vertebra three through 15, an area approximately one meter long and half a meter wide, the details of which are shown in Fig. 1B. These remains are identified as gut-content based on the pattern of bone and tooth erosion, the physical arrangement of individuals and elements, and their relationship to the articulated predator's body, preserved in the region known to house the stomach in extant lizards (Srichairat et al., 2018). The preservation of the gut-content is generally good, and it appears digestion was halted relatively soon after the meal was taken, preserving large portions of the individual elements of the prey items. There is no evidence of shark scavenging on the prey items; however, it is possible that some prey items were lost due to scavenging, complete digestion, or non-fossilization.

Although some mixing has occurred, the prey items are largely segregated taxonomically in the sequence in which they were consumed (Fig. 1B). In the most posterior part of the stomach mass are portions of the skull and mandible of a *Gavialimimus* sp. (MGUAN PA 183B). There are also portions of the snout and the left squamosal of the mosasaurine that is largely preserved in the most anterior part of the gut (MGUAN PA183D), but those are situated and preserved in such a way that they were likely transported there once the visceral cavity of the consumer was breached. What are now recognized as gut-content, were largely covered in matrix at the time of the field excavation, and were not recognized as such. Consequently, the area containing the gut-content was taken as two blocks (Fig. 1B), and the anterior portion of the snout of a *Prognathodon kianda* (MGUAN PA 183C) was found while trenching, between the main concentrations of the two other taxa. Thus, there is not the same level of detail in mapping these elements as the remainder of the specimen (Fig. 1A, B). In the most anterior part of the stomach region is a partial skull, mandibles, and some postcrania of a small mosasaurine (MGUAN PA183D), which represents a new taxon, which is named, diagnosed, figured, and described in the present contribution.

SYSTEMATIC PALEONTOLOGY

Order SQUAMATA Oppel, 1811
Family MOSASAURIDAE Gervais, 1852
Subfamily PLIOPLATECARPINAE Dollo, 1884
Genus *GAVIALIMIMUS* Strong et al., 2020
GAVIALIMIMUS sp.

Referred specimen — MGUAN PA 183B (Fig. 3A, B)

Locality, Horizon, and Age — The specimen was collected

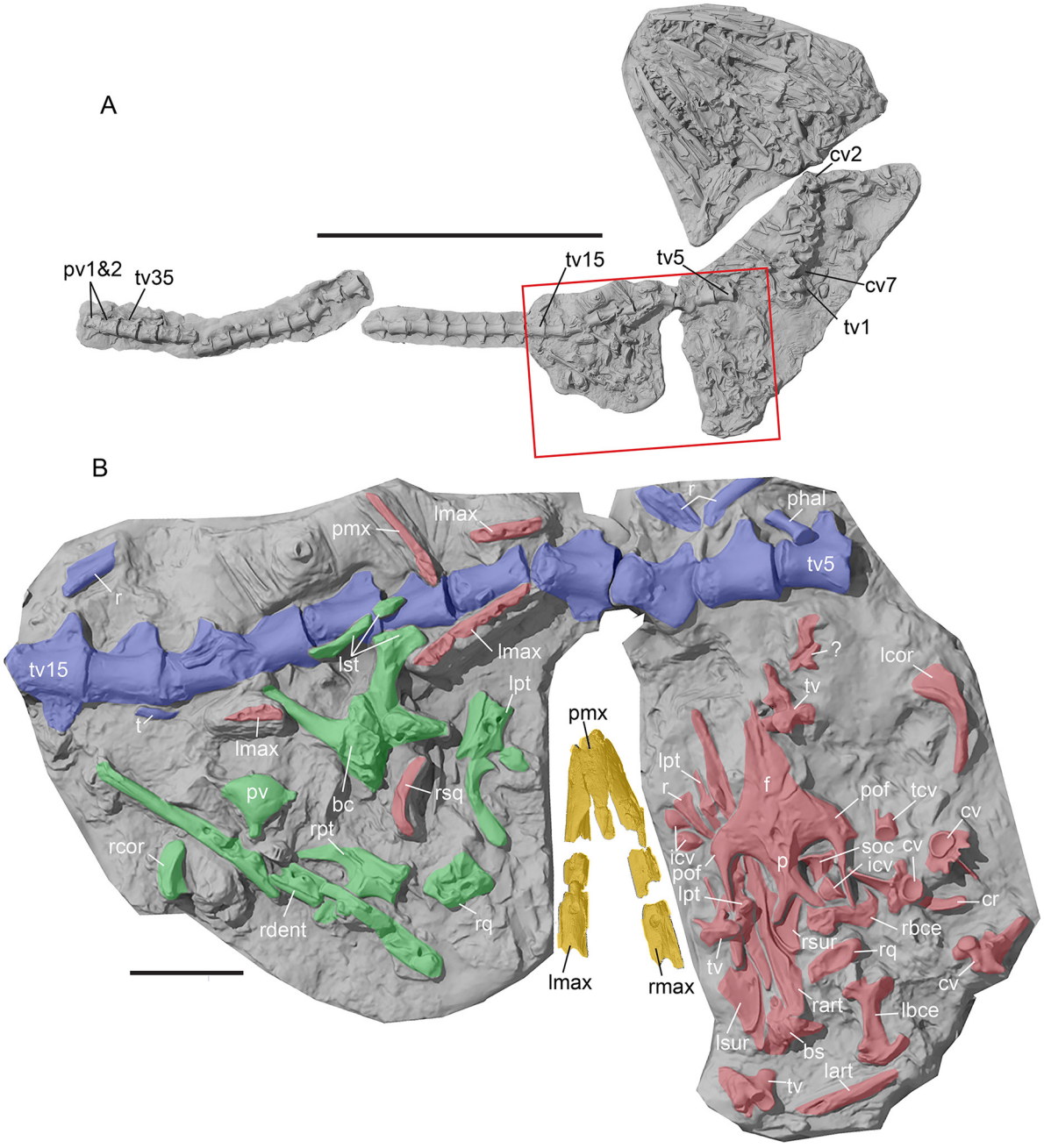

FIGURE 1. Overview of preservation orientation of predator and prey items. **A**, position of the primary field jackets of a semi-articulated skeleton *Prognathodon kianda* (MGUAN PA183) with rectangle denoting location of prey items; **B**, detail of stomach region with prey items. Bones colored blue are those of the predator *Prognathodon kianda* (MGUAN PA183). Prey items are *Gavialimimus* sp. (MGUAN PA183B) identified by green shading, *Prognathodon kianda* (MGUAN PA183C) in yellow, and *Bentiabasaurus jacobsi* gen. et sp. nov. (MGUAN P183D) in red. Note that disarticulated elements of MGUAN PA183C were removed in the field as hand samples while separating the two main blocks containing the gut-content, and therefore the position of the rearticulated elements as shown is conjectural. Additional elements of MGUAN PA183 (e.g., premaxilla, palatines, rib fragments, trunk vertebrae 2-4, 2 pygal vertebrae) were collected in the field as hand samples and smaller blocks and are not shown in this figure. **Abbreviations: cv**, cervical vertebra; **bc**, braincase; **bs**, basisphenoid; **f**, frontal; **icv**, indeterminate caudal vertebra; **lart**, left articular; **lbce**, left braincase elements; **lcor**, left coronoid; **lmax**, left maxilla; **lpt**, left pterygoid; **lst**, left supratemporal; **lsur**, left surangular; **p**, parietal; **pmx**, premaxilla; **phal**, phalanx; **pv**, pygal vertebra; **r**, rib; **rart**, right articular; **rbce**, right braincase elements; **rcor**, right coronoid; **rdent**, right dentary; **rmax**, right maxilla; **rpt**, right pterygoid; **rq**, right quadrate; **rsq**, right squamosal; **rsur**, right surangular; **soc**, supraoccipital; **t**, tooth; **tcv**, terminal caudal vertebra; **tv**, trunk vertebra. Scale bars equal 1 m for A and 10 cm for B.

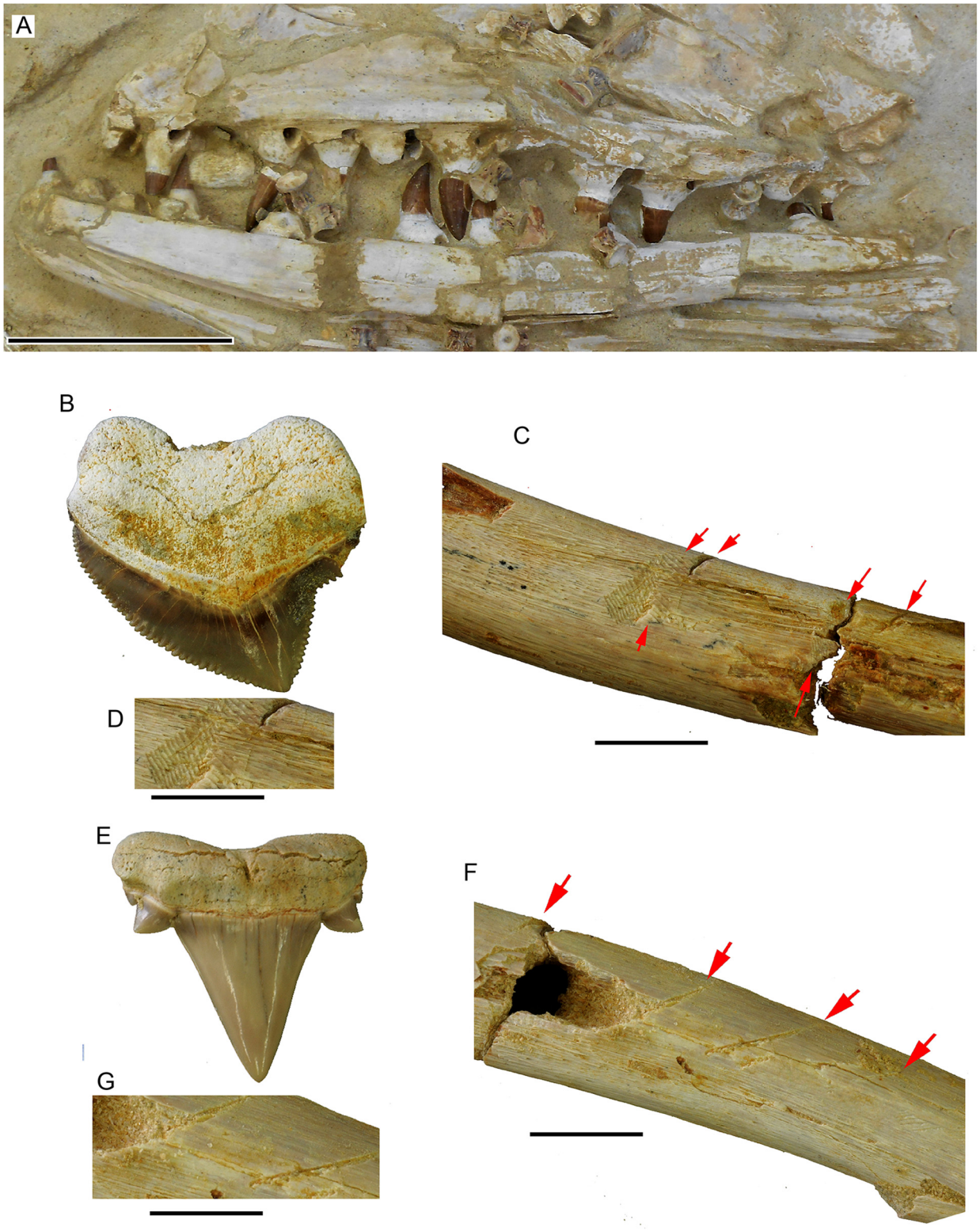

FIGURE 2. Typical preservation of the predator, *Prognathodon kianda* (MGUAN PA183) with examples of taphonomic modifications. **A**, detail of right maxilla and dentary showing preservation of bone and tooth surfaces; **B**, tooth of *Squalicorax pristodontus;* **C**, typical scavenging marks on rib section of predator by *Squalicorax pristodontus*; **D**, detail of same; **E**, tooth of *Cretalamna* sp.; **F**, typical scavenging marks on rib section of predator by *Cretalamna* sp.; **G**, detail of same. Arrows point to scavenger marks. Scale bar for A equals 10 cm, and for B-F scale bar equals 1 cm.

at Bentiaba, Angola, approximately one meter above "Bench 19" of Strganac et al. (2015a), falling within magnetochron 32n, a period of about 240 kyr, between 71.40 and 71.64 Ma (Strganac et al., 2014; 2015a).

DESCRIPTION

Preservation

The specimen MGUAN PA 183B, here identified as *Gavialimimus* sp., is the most posterior of the three concentrations of bone found in the stomach region of the predator. It preserves parts of the skull and right mandible, including the fragmentary right quadrate, dentary, squamosal, the articulated braincase, the left coronoid, both pterygoids, and a single anterior caudal vertebra. Once prepared to the point seen in Fig. 1, the orientation of all of the elements was captured with photography, silicone mold making and casting, and 3d scanning, and subsequently, the individual elements were removed and prepared for study. All of the elements referred to this taxon were found in close proximity to one another (Fig. 1B, highlighted in green). There are no repeating elements, and most of those preserved are positioned relative to one another approximately as they would have been in life, though there is anterior displacement of the quadrate and anterior and rightward displacement of the coronoid. Taking the orientation of the braincase as defining the midline, the right and left elements are largely preserved on their respective sides. We therefore interpret the skull elements and mandible parts are a single individual; however, the unexpected association of the anterior caudal (pygal) vertebra with the skull elements cannot rule out that it is a remnant of another meal, so our acceptance of it here as being part of this animal is tentative.

Skull

Braincase — The braincase is largely complete, but cracked and component elements displaced, and some postdepositional crushing is apparent. The occipital condyle makes up most of the vertebral articulation, with the otooccipitals contributing minimally. The basal tubera are more or less ventrally oriented in posterior view and tall and narrow in lateral view. Their posterior lateral surface is largely covered with the inferior process of the otoccipital. Their anterior faces are extensively overlapped by the posterior parts of the basisphenoid.

The basisphenoid is somewhat crushed and broken but complete. In ventral view, it is broad posteriorly where it articulates with and overlaps the basioccipital, and narrows substantially anteriorly. The basipterygoid processes are short and narrow and directed anterolaterally and trend anteroventrally. On the ventral surface, between the basipterygoid processes, is a groove and within it a low narrow ridge originates, continuing anteriorly along the centerline of the convex ventral surface of the parasphenoid rostrum. Above, the parasphenoid rostrum is concave, its edges converging anteriorly to form a point. Further posterior, the sella turcica is not well preserved and is damaged posteriorly, exposing an internal canal for the so-called basilar artery, behind which is the floor of the medullary cavity, suggesting it would have possessed a relatively short dorsum sellae. The exits for the carotid and cerebral carotid arteries are not discernable.

The otooccipitals, prootics, and supratemporals are in articulation but slightly cracked and displaced. The inferior process of the otoccipital forms a crista tuberalis posterolaterally, medial to which there is a recess for the foramina for nerves X, XI, and XII, similar to the condition in *Platecarpus* (Russell, 1967). Anteriorly the oval and round windows are obscured. The prootics are nearly complete, but again, broken and some fragments displaced. There is a large anterior notch for nerve V, overhung by a long anterodorsal process. Nerve VII appears to exit on the posterior part of the lateral face of the inferior process of the prootic, and runs anteroventrally in a shallow groove. The supraoccipital forms a relatively flat surface posteriorly and rises anteriorly, but preservation limits further description. Both the right and left supratemporals are present but broken, but the left is relatively complete. The anteroventral part of the supratemporal is deeply sandwiched between the paroccipital processes medially and the posterodorsal ramus of the prootic laterally. Proximally, in lateral view the supratemporal expands and is somewhat T-shaped. The dorsal part forms an anteriorly trending raised ridge.The ventral part is flat, forming a large posteroventral process, below which is part of the ventrally facing articulation for the quadrate. Though broken and displaced slightly (Fig. 1B), the anteromedial process of the supratemporal that articulates with the parietal is preserved. This process is rod-like, but distally, it thins and expands laterally, and would have inserted between the horizontally bifurcated distal parietal ramus (MJP personal observation). Additionally, raised edges lateral to the articulating surface limit angular motion at this joint, rendering it akinetic. This novel supratemporal-parietal articulation

appears to be unique to this taxon.

Squamosal — The posterior part of the right squamosal was recovered below the braincase during removal of the elements from the field jacket. It is somewhat hatchet-shaped with a short dorsal process and a broad, distally expanding ventral process that articulates with the quadrate. The dorsal slot-like articulation for the posterior ramus of the postorbitofrontal terminates anterior to the quadrate articulation.

Quadrate — The right quadrate is more complete than the one described by Strong et al. (2020), but the surface is somewhat decalcified, and it is missing the alar rim. The basal portion, including the mandibular condyle, is badly eroded. The suprastapedial process is long, about two-thirds the total height of the quadrate. The dorsal part of the suprastapedial process has nearly parallel sides, and it broadens distally reaching its maximum breadth where it meets the so-called infrastapedial process. The stapedial pit is broadly oval and inclined posterodorsally, and lies between the narrow dorsal medial ridge anterodorsally, and partly overlying the auditory meatus (stapedial notch of Strong et al., 2020). There is a marked posterodorsal inflection of the narrow medial ridge at the level of the stapedial pit. A deep sulcus originates just below the stapedial pit, trending posteroventrally while broadening, and terminating at the level of the juncture of the suprastapedial and infrastapdial processes. The comparable aspects of the quadrate are nearly identical to those of Strong et al. (2020, their figure 8).

Pterygoids — The main body of the pterygoid is flat and broad and the tooth row lies slightly medially, and does not extend posteriorly beyond the posterior margin of the ectopterygoid process. The ectopterygoid process is obscured by the dentary above, but has a broad base and extends laterally. In ventral view, there is an incomplete ectopterygoid, displaced slightly from its extensive sutural articulation with the ectopterygoid process. Posteromedially, a thin, slightly oval, rod-like basisphenoid process leaves the main body of the pterygoid and a more robust quadrate ramus posterolaterally. Neither are complete distally. Both pterygoids appear to have been truncated anteriorly, each preserving only three tooth positions. Other pterygoid specimens of this taxon from the locality are also incomplete anteriorly, but demonstrate a minimum of 5 tooth positions (MGUAN PA 551).

Dentary — The posterior dentary bears a long edentulous portion about five tooth positions long, and the dentigerous part preserves space for 10 tooth positions, but there are portions where the alveolus is completely eroded. It is not clear if it is complete anteriorly. Teeth are completely eroded to their bases and there are no preserved replacement teeth. The most posterior eroded tooth bases are elongate, suggesting laterally compressed dentition whereas the more anterior ones are more nearly oval to circular. Resorption pits are present posteromedial to eroded tooth bases. There are clear accommodation pits (interdental pits of Strong et al., 2020) anterolateral to the third from last and the fifth from last tooth positions. The medial parapet is taller than the lateral wall of the dentary.

Coronoid — Only the anterior part of the coronoid is preserved. There is no anterior bifurcation in dorsal view. In lateral view, the dorsal margin rises quickly, suggesting a tall, short coronoid such as that seen in *Selmasaurus johnsoni* (Polcyn and Everhart, 2008). The ventral articulation with the surangular is only slightly concave.

Taxonomic remarks — Based on comparison with the holotype material (MHNM.KHG.1231), the specimen (MGUAN PA183B) can be confidently referred to the genus *Gavialimimus* (Strong et al., 2020) on the basis of the long edentulous posterior portion of the dentary, presence of accommodation pits anterolateral to tooth positions, the tall medial parapet, the positionally controlled geometry of teeth, and tentatively, the reconstructed tooth count. This referral is also supported by characters of the quadrate, including the distally expanded suprastapedial process.

Subfamily MOSASAURINAE Gervais, 1852
Tribe GLOBIDENSINI Bell, 1997
PROGNATHODON KIANDA Schulp et al. 2008

Referred specimen — MGUAN PA 183C (Fig. 3C-J, see also Strganac et al., 2015).

Locality, Horizon, and Age — As for MGUAN PA183B above.

DESCRIPTION

Preservation

The preserved portion of the skull is represented by the anterior part of the premaxilla and portions of both maxillae. The external surfaces are badly decalcified, removing the anterior end of premaxilla, much of the cortical bone of all elements, and the tooth crowns. Conversely, the internal

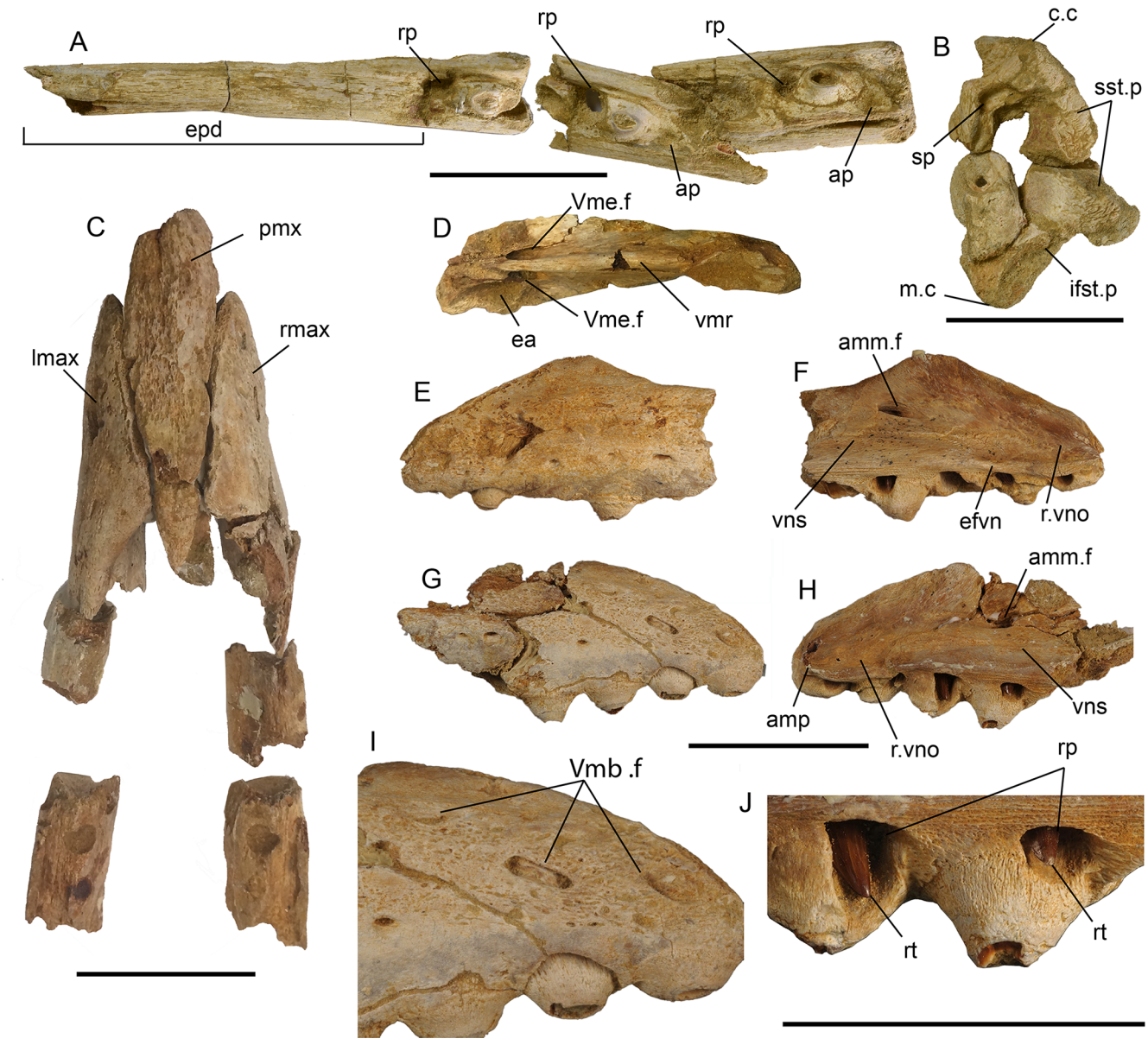

FIGURE 3. Preservation of prey items *Gavialimimus* sp. (MGUAN PA 183B) and *Prognathodon kianda* (MGUAN PA183C). **A**, *Gavialimimus* sp. (MGUAN PA183B) posterior right dentary in dorsal view; **B**, right quadrate of the same in medial view; **C**, *Prognathodon kianda* (MGUANPA183C), rearticulated snout fragments in dorsal view; **D**, premaxilla of same in ventral view; **E**, anterior left maxilla fragment of same in lateral and **F**, medial views; right maxilla fragment of same in **G**, lateral and **H**, medial views; **I**, details of anterior part of right maxilla fragment in lateral view; **J**, detail of posterior part of right maxilla fragment in medial view. **Abbreviations: amm.f**, anteromedial maxillary foramen; **amp**, anteromedial process; **ap**, accommodation pit; **c.c**, cephalic condyle; **efvn**, emargination for the fenestra vomeronasalis; **epd**, edentulous posterior dentary; **lmax,** left maxilla; **ifst.p**, infrastapedial process; **m.c**, manibular condyle; **pmx**, premaxilla; **rmax**, right maxilla; **rp**, resorption pit; **rt**, replacement tooth; **r.vno**, recess for vomeronasal organ; **sp**, stapedial pit; **sst.p**, suprastapedial process; **Vmb.f**, foramen for maxillary branch of trigeminal nerve; **Vme.f**, foramen for medial ethmoidal branch of trigeminal nerve; **vns**, vomeronasal sulcus. Scale bars equal 5 cm.

surfaces, including the maxillary premaxillary articulation surfaces, are well preserved and show no damage, suggesting the anterior snout was still intact during digestion.

Skull

Premaxilla — The premaxilla is badly decalcified anteriorly, missing the rostrum and the anterior tooth positions, but

retaining portions of the resorption pits for those (Fig. 3). The posterior alveoli are empty, their anterior walls trending anteroventrally, and their lateral walls breached by erosion (Fig. 3C, D). The posterior teeth were apparently in late stage replacement as the teeth were not ankylosed within the alveoli and there is no sign of resorption pits. Medially, between the posterior tooth positions, is the remnant of an elevated incisive process, bearing a central groove lateral to which are parasagittal ridges. The parasagittal ridges of the process trend posteriorly, terminating just at the anterior rim of the foramen for the medial ethmoidal nerve. The ventral medial ridge begins between the parasagittal ridges, just medial to the center of the posterior tooth positions and just below the level of the incisive process. The foramina for the medial ethmoidal nerve are far anterior, just posteromedial to the posterior tooth positions, in the posterior wall of the dentigerous portion of the premaxilla. The foramina are separated by a relatively low ventral medial ridge, posterior to which the ridge protrudes from the apex of a somewhat triangular cross section of the posterior process. On either side of the posterior process are well preserved maxillary articulation surfaces showing fine ridges and textures associated with soft tissues. The posterior process protrudes about 2 cm into the internarial space but is eroded and missing posterior to this. In dorsal view, the cortical bone is mostly gone, exposing trabecular bone, except for some small patches on the anterior right side (Fig. 3C).

Maxillae — Each maxilla, though fragmentary and badly eroded, preserves ten tooth positions. The anterior part of both maxillae is well-preserved medially, but their external surfaces are badly eroded. Anteriorly, at the ventral part of the medial parapet, the anteromedial process is preserved on the left maxilla. Posterior to that, there is an emargination for the fenestra vomeronasalis, running posteriorly to a point one-third of the third tooth position. Dorsal to this emargination is a recess for the vomeronasal organ, and at a point dorsal to the posterior terminus of the emargination, a sulcus we term the "vomeronasal sulcus", which originates on the posterior border of the recess for the vomeronasal organ, and runs posteriorly, trending slightly laterally. Dorsal to the posterior half of the recess for the vomeronasal organ is another small sulcus we take to receive the lateral part of the septomaxilla or associated soft tissue. The maximum height of the maxilla is dorsal to a point between the third and fourth tooth positions, posterior to which lies a well-defined narial emargination. Above the fourth tooth position, near the narial emargination, is the anteromedial maxillary foramen, homologous with the dorsal maxillary foramen of Bahl (1937). As with the premaxilla, the external surfaces of the maxillae are badly eroded (Fig. 3E, G), and significant portions of the cortical bone are missing. Interestingly, the area just above the teeth and just anterior to the external nares, preserves the cortical bone, possibly indicative of thicker and/or more resistant soft tissue in those areas. The lateral central part of both maxillae is eroded, exposing trabecular bone. The foramina for the maxillary branch of trigeminal nerve are eroded and opened to reveal the underlying canals (Fig. 3I). The erupted and ankylosed marginal teeth are all eroded, but replacement teeth are perfectly preserved within the resorption pits. Judging from the eroded tooth bases, the anterior tooth cross sections are nearly circular and more posterior teeth increasingly laterally compressed.

Taxonomic remarks — The specimen is confidently referred to *Prognathodon kianda* by comparison with other individuals in the MGUAN PA collection (e.g., MGUAN PA 129 [holotype], PA 25, PA 183, PA 271). These specimens were all collected within a limited geographic area and at essentially the same stratigraphic level (Strganac et al., 2015a) and no other *Prognathodon* species have been recovered at the locality. The far anterior position of the ethmoidal foramina, the position and nature of the external nares, the dorsal shape of the premaxilla, the nature of the tooth implantation and replacement pattern, are all identical to the comparative specimens. Nonetheless, the individual described here (MGUAN PA 183C) is smaller than the holotype and referred specimens of *P. kianda*, and some ontogenetic differences are apparent. For instance, the slope of the anterior maxillary premaxillary suture is relatively low compared to larger individuals of *P. kianda*. We quantify this by measuring the relative height of the anterior snout (distance on lateral side from its tallest anterior point to the ventral margin) compared to the distance between the centers of the bases of the first four teeth (Fig. 4). The larger individuals all range between ~0.9 and ~1.0, whereas PA 183C is ~0.7. An individual of intermediate size between PA 183C and PA 183, is ~0.8. There is a general trend toward a relatively taller, higher sloped suture through the ontogeny of *P. kianda*, but with a downward shift in the ratio for the largest individual (PA 271) at ~0.9. However, that individual has 12 tooth positions, versus 13 in the rest of the sample of

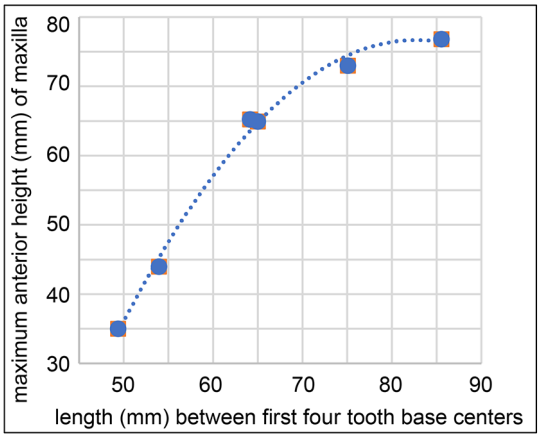

specimen	length	height	ratio	tooth count
PA183C	49.47	35.00	0.71	?
PA25	53.93	43.95	0.81	13
PA13	64.97	64.92	1.00	13
PA183	64.11	65.22	1.02	13
PA129	75.05	73.00	0.97	13
PA271	85.53	76.83	0.90	12

FIGURE 4. Ontogenetic maxillary growth. All measurements in millimeters. Curve fit is second order polynomial.

complete maxillae, and thus changes in tooth spacing may in part account for this difference in the ratio. In any event, when plotted (Fig. 4), these data can be interpreted as allometric growth, with height increasing faster than length, and the relative increase in height slowing as the individual ages. Another example of ontogenetic change, taken from the specimen described here, can be seen in the ventral medial ridge. While the ridge is low and robust in PA 183C, in the larger specimens that preserve it (PA 183, PA 129), it is increasingly thinner and their height correlates with the relative height increase of the snout in older (larger) individuals. A third but related example, is the increased distance between the level of the ethmoidal foramina entrances and the level of the incisive process, as the premaxilla grows taller. Though preliminary, these observations demonstrate the potential of the Projecto PaleoAngola collection for the understanding of ontogenetic change in at least *Prognathodon kianda*, which will be addressed elsewhere. Notwithstanding the ontogenetic differences noted above, we consider MGAUN PA 183C a relatively young individual of *Prognathodon kianda*, and thus the first report of cannibalism in mosasaurs.

Tribe PLOTOSAURINI Bell 1997

BENTIABASAURUS JACOBSI gen. et sp. nov.

(Figs. 1,5,6,7,8,9,10,11,12, and 13)

Syntypes — MGUAN PA 183D, recovered from the most anterior part of the gut-content, and thus the predators last meal, includes a partial skull, partial mandibles, four cervical vertebrae, two cervical ribs, six trunk vertebrae, and five caudal vertebrae; MGUAN PA554, partial mandibles and quadrates.

Referred specimens — MGUAN PA 282, MGUAN PA 283, and MGUN PA 284, all partial right quadrates.

Locality and horizon — All of the specimens except MGUAN PA 554 were collected within the first two meters above "Bench 19" of Strganac et al. (2015). The exception, MGUAN PA 554, was collected approximately 10-12 meters above "Bench 19", but included in the interval which is constrained to magnetochron 32n, a period of about 240 kyr, between 71.40 and 71.64 Ma (Strganac et al., 2014; 2015a).

Etymology — The genus name is a combination of Bentiaba, for the locality that produced the specimens, and to honor the people of Bentiaba, Angola, and the Greek "*saurus*" for lizard. The species epithet is in honor of Louis L. Jacobs for his many contributions to African vertebrate paleontology. He is the consummate vertebrate paleontologist, explorer, ambassador, teacher, mentor, and friend.

Diagnosis — A gracile mosasaurine of the tribe plotosaurini possessing the following unique combination of characters: premaxilla with foramen for medial ethmoidal nerve enters posterior process between the second and third maxillary tooth position, minimum of 15 maxillary teeth (14 present and one additional posterior tooth estimated), a distinct ventromedial facing groove on the medial side of maxilla parapet, frontal subtriangular and narrow with concave lateral margins, frontal posterior parasagittal tabs closely embrace a relatively large pineal foramen, anterior parietal table elongate and triangular with posterior margins that diverge sharply, postorbitofrontal-parietal suture angular and z-shaped, prootic with cranial nerve VII exit on lateral surface of inferior process, quadrate laterally narrow, blunt poster-oventral ascending rim, well developed alar groove, distinct vertical groove on anteromedial quadrate face at mid-height, pterygoid tooth row on straight elevated process, dentary with 15 or 16 tooth positions (13 present and room for two

or three additional estimated), surangular with high coronoid buttress, retroarticular projects posteriorly without ventral or medial deflection, coronoid with posterior notch in medial flange, medial flange only slightly deeper than lateral flange and does not contact angular, marginal dentition symmetrically bicarinate, laterally compressed, with smooth enamel surface, zygosphenes-zygantra present through at least thoracic vertebrae, and fused hemal arches on caudal vertebrae.

Taxonomic comments — *Bentiabasaurus jacobsi* gen. et sp. nov. can be differentiated from all other mosasaurs by the unique combination of characters noted in the diagnosis. It can be confidently referred to mosasaurinae by possession of a narrow, straight and elevated pterygoid tooth row, coronoid concave above with greatly expanded posterior wing, rapidly rising high thin surangular-coronoid buttress, anterior vertebral condyles nearly circular and essentially equidimensional, and fused caudal hemal arches. Though it retains some relatively plesiomorphic mosasaurine characters (e.g., smooth, symmetrically bicarinate and laterally compressed teeth; narrow triangular frontal; and well-developed zygosphenes and zygantra in trunk vertebrae), it can be referred to the tribe Plotosaurini (*sensu* Bell, 1997) by possession of a prominent medial maxillary groove, large parasagittal frontal tabs embracing pineal foramen, and a quadrate with deep alar groove and accessory medial ridge. The mosaic of plesiomorphic and derived characters present in *Bentiabasaurus jacobsi* gen. et sp. nov. separate it from other known Plotosaurini.

Furthermore, the position of the exit for cranial nerve VII in *Bentiabasaurus jacobsi* gen. et sp. nov. is unique among Plotosaurini with a single exception, a specimen referred to *Mosasaurus dekayi* (Bronn, 1838) by Russell (1967 p. 138). That specimen (YPM 1582), preserves a tooth, the posterior part of the parietal, and a fragmentary left prootic, which bears a similar position of the exit for cranial nerve VII. However, in that specimen, the preserved tooth, though "more or less" symmetrically bicarinate, is significantly more robust and highly faceted, and the margins of parietal surface slightly converge at their posterior termination. These two latter characters are unlike the morphology of *Bentiabasaurus jacobsi* gen. et sp. nov. (MGUAN PA 183D) and thus any relationship with *M. dekayi* is rejected.

Two of the characters noted above, the prominent medial maxillary groove and the accessory medial ridge of the quadrate, have not been previously used to diagnose Plotosaurini. Both characters are present in the holotype and referred specimens of *Mosasaurus hoffmanni,* referred specimens of *Mosasaurus* cf. *M. conodon* (e.g., SMU 76348, SMU 76836), and verified in CT data of the holotype of *Plotosaurus bennisoni* (DigiMorph.org). The medial maxillary groove has not been verified in the holotype of *Mosasaurus missouriensis*, but that specimen does possess the accessory medial ridge of the quadrate, although it is slightly damaged. It is present in referred specimens of that taxon (Konishi et al., 2014; their figure 5). Neither character is present in *Clidastes* or *Prognathodon* and related forms (MJP personal observations), and thus appear to be useful to diagnose Plotosaurini.

Recently, Zietlow et al. (2023) described *Jormungandr walhallaensis* (NDGS 10838) from the middle Campanian of North Dakota, which also possesses a mosaic of plesiomorphic and derived mosasaurine characters, including some it shares with later diverging plotosaurins, including the medial maxillary groove, and the deep alar groove of quadrate, but is unlike that of *Bentiabasaurus jacobsi* gen. et sp. nov. in that its quadrate does not possess any posterior projection of the infrastapedial process, nor does it possess an accessory medial ridge, but uniquely possesses a deep posteroventral medial sulcus (Zietlow et al., 2023, their figure 24).

DESCRIPTION

Specimens and preservation

Bentiabasaurus jacobsi gen. et sp. nov. is described primarily from MGAUN PA 183D, with supplementary description of the quadrate, dentary, coronoid, and marginal dentition from MGUAN PA 554. Additional data is also derived from quadrate specimens MGUAN PA 282, MGUAN PA 283, and MGUAN PA 284. The largest concentration of MGUAN PA 183D is in the anterior part of the gut of a specimen of *Prognathodon kianda* (MGUAN PA 183), and probably represents the last meal of the predator. The left squamosal, premaxilla and maxillae fragments are displaced posteriorly in the region of MGUAN PA 183B (hindgut) with the premaxilla and maxillary fragments lying upon and adjacent to the vertebrae of the predator (Fig. 1B). The frontal, parietal, and postorbitofrontals are in articulation, the braincase and quadrates disarticulated but in close proximity, and the left pterygoid and partial mandibles, lying below the bone mass. Mixed with this concentration are both trunk and caudal vertebrae, and the cervical vertebrae and additional trunk and caudal vertebrae were recovered in close proximity.

The partial quadrates and mandibles of MGUAN PA 554 were recovered about two hundred meters from MGUAN PA 183 and about ten meters higher in the section. The specimen suffered severe weathering at the surface, with significant bone loss and breakage, but is included here as the primary source of data on the dentaries and marginal dentition. The partial quadrates (MGUAN PA 282, MGUAN PA 283, and MGUAN PA 284) were isolated finds at the weathered surface and all within the first two meters above Bench 19.

Skull

Premaxilla — The nearly complete premaxilla is present (Fig. 5A-F). Its dorsal and dentigerous sections are partially digested, but the post-dentigerous ventral part is well preserved, suggesting it may have been protected from stomach acids by soft tissue or was in articulation with the maxillae for some time after ingestion. In dorsal view (Fig. 5A), most of the cortical bone is missing. The dentigerous part is eroded to the point that the bases of the anterior alveoli are exposed. The lateral margins of the posterior process are nearly parallel, gradually diverging slightly posteriorly. Nothing can be said of the suture with the maxilla due to decalcification. In ventral view, the anterior and posterior tooth bases and resorption pits can be seen, and tooth bases suggest they supported laterally compressed crowns. The vomer processes are prominent and there is a deep groove between them that extends anteriorly, its margins converging. The medial ethmoidal nerve enters on the ventral posterior process at approximately the second or third maxillary tooth position. A narrow, prominent ventral medial ridge originates at or near the posterior base of the dentigerous portion, extending posteriorly and deepening slightly.

Maxilla — The left maxilla is present, but broken into three pieces (Fig. 5G-K, Q). There is a small fragment of the anterior part of the right maxilla (Fig. 5L-P). Judging by comparison with complete and better-preserved specimens of *Mosasaurus* and related forms, nearly the entire length of the left maxilla is present, missing only a small posterior portion. There are 14 tooth positions, and room for at least one more in the missing posterior section. There is a prominent groove or gutter on the medial side of the parapet, which runs from about the fifth to about the 11^{th} or 12^{th} tooth position becoming shallower and less distinct at the anterior terminus of the palatine articulation on the posterior fragment (Fig. 4G). The palatine articulation is a thin blade-like process that projects dorsomedially high on the posterior parapet, rising at about the 12^{th} or 13^{th} tooth position. All eroded tooth bases in the maxilla suggest the crowns were laterally compressed. There are two replacement teeth preserved in the anterior maxillae fragments. They are laterally compressed and possess smooth enamel surfaces with no fluting or facets, and their tips are digested.

Frontal — The frontal is heavily decalcified dorsally, but preserves the overall shape and is mostly complete, except for the very anterior part (Fig. 6). It is subtriangular and narrow, measuring ~113 mm midline length and ~84 mm between the posterolateral alae (L:W=1.35). The lateral margins are slightly concave, arcuate posteriorly. Anteriorly, the margins appear to step in medially, then converge slightly. Though eroded, there is a remnant of an anterior median ridge preserved. The posterior parasagittal tabs of the frontal are large and triangular, together are 34.6 mm wide, occupying about 41% the posterior width between the posterolateral alae. They closely embrace a relatively large pineal foramen medially, and only a narrow band of bone on the parietal that surrounds the pineal foramen, is exposed between them. The broadly triangular posterolateral alae trend more lateral than posterior. Posteriorly, the posterior margin of the posterolateral ala and the lateral margin of the parasagittal tab, meet at an angle of about 110^{o}. Ventrally, most of the frontal is obscured by overlying bone (Fig. 7), exposing only the anterior part. The surface preservation is good and shows no sign of erosion. The olfactory canal is relatively broad anteriorly, bounded by descending processes that are parallel anteriorly and converge posteriorly. The ventral rim of the posterior part of the descending process thins to a crest, and then expands slightly and bears a sulcus, interpreted here as the solium supraseptale. Anteriorly the descending processes are broad and rounded over, and they also slope down to meet the ventral surface of the frontal anteriorly, and bear longitudinal striations. There is no evidence of an anterior ventral medial ridge within the olfactory canal.

Parietal — The parietal is complete, but the dorsal surface partially digested. A pit to the right of and posterolateral to the pineal foramen is field damage that occurred during excavation. The posterolateral rami, and portions below the parietal table and within the supratemporal fenestrae are well preserved with no erosion, and were likely protected from stomach acids by muscle and connective tissue. Anteriorly, a large, slightly elongate pineal foramen is closely embraced by

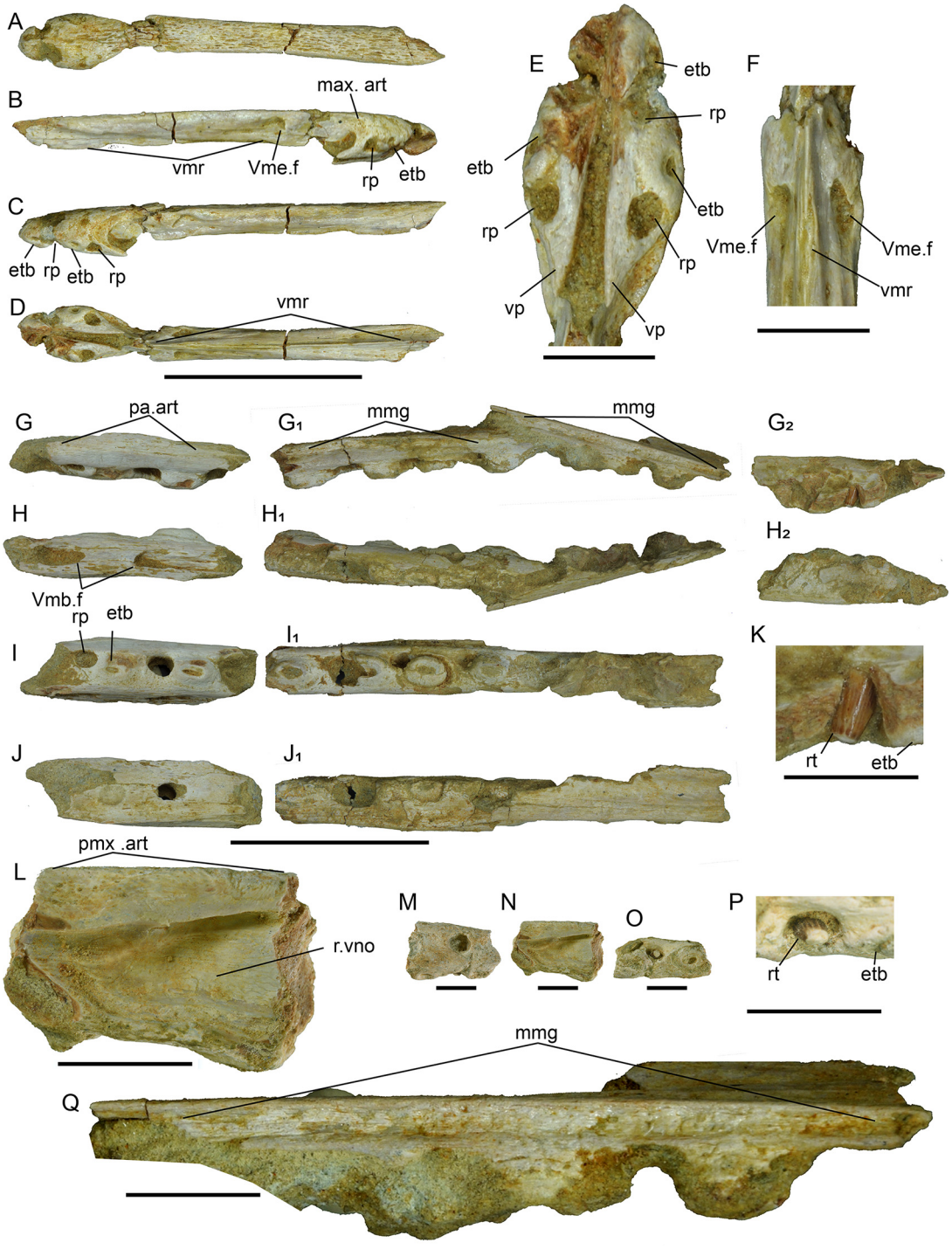

FIGURE 5. Snout elements of *Bentiabasaurus jacobsi* gen. et sp. nov. (MGUAN P183D). **A**, premaxilla in dorsal, **B**, right lateral, **C**, left lateral, and **D**, ventral views; **E**, ventral detailed view of dentigerous part of premaxilla; **F**, ventral detailed view of post-dentigerous part of premaxilla; **G**, left maxilla in medial, **H**, lateral, **I**, ventral, and **J**, dorsal views; **K**, detail of replacement tooth in G_2; **L**, anterior fragment of right maxilla in medial view; **M**, same in dorsal, **N**, medial and **O**, ventral views. **P**, detail of replacement tooth in O; **Q**, detail of anterior part of G_1 showing prominent medial groove. **Abbreviations: etb**, eroded tooth base; **max.art**, maxillary articulation; **mmg**, medial maxillary groove; **pa.art**, palatine articulation; **pmx.art**, premaxillary articulation; **rp**, replacement tooth; **r.vno**, recess for vomeronasal organ; **Vmb.f**, foramen for maxillary branch of trigeminal nerve; **Vme.f**, foramen for medial ethmoidal branch of trigeminal nerve; **Vme.f**, foramen for medial ethmoidal branch of trigeminal nerve; **Vmr**, ventral median ridge; **Vp**, vomer process. Scale bars equal 5 cm for A-D, and G-J. Scale bars for all others equals 1 cm.

FIGURE 6. Main skull block of *Bentiabasaurus jacobsi* gen. et sp. nov. (MGUAN P183D) from above. **A**, skull roof, palatal elements, partial mandibles, braincase elements, and quadrate from above; **B**, same, rendered isosurface model derived from threshold-segmented of CT scan data. **Abbreviations: ct.f**, foramen for the chorda tympani; **f**, frontal; **lart**, left articular; **lsur**, left surangular; **p**, parietal; **pof**, postorbitofrontal; **rart**, right articular; **rbce**, right braincase elements; **rcor**, right coronoid; **rpt**, right pterygoid; **rq**, right quadrate; **rsur**, right surangular; **soc**, supraoccipital; **tcv**, terminal caudal vertebra; **tv**, trunk vertebra. Scale equals 10 cm.

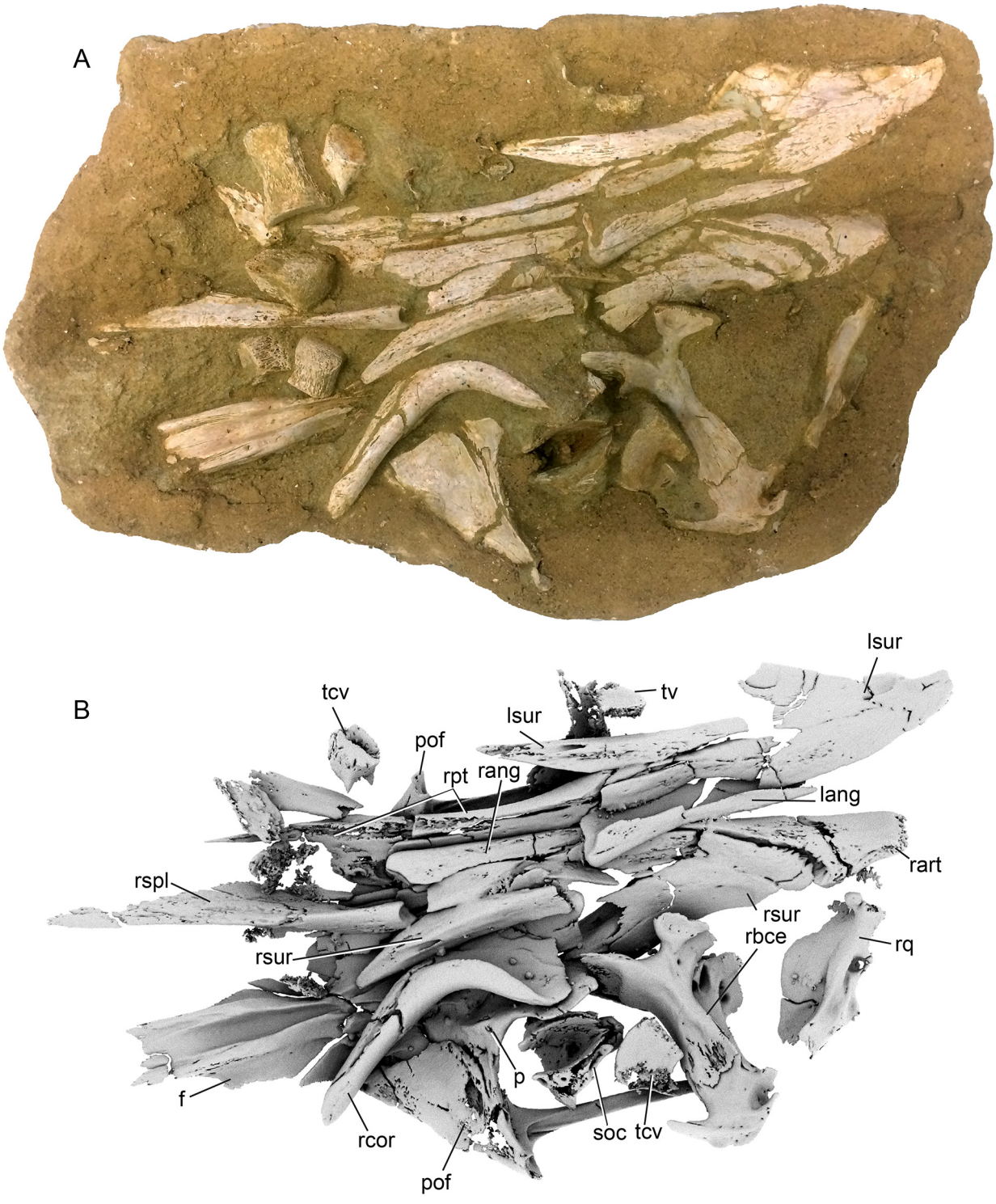

FIGURE 7. Main skull block of *Bentiabasaurus jacobsi* gen. et sp. nov. (MGUAN P183D) from below. **A**, skull roof, palatal elements, partial mandibles, braincase elements, and quadrate from below; **B**, same, rendered isosurface model derived from threshold-segmented of CT scan data. **Abbreviations:** as in Figure 5. Scale equals 10 cm.

parasagittal posterior tabs from frontal. The foramen is completely within the parietal. Laterally, the parietal meets the postorbitofrontal in an angular, z-shaped suture, inset medially from the posterolateral alae. The parietal is ~61 mm long measured along the midline from the anterior margin of the pineal foramen. In dorsal view, the anterior lateral margins of the triangular parietal table are nearly straight, converging posteriorly, and reaching their narrowest point at the anterior terminus of the posteromedial fossa, or about 71% posterior midline length of the parietal (measuring ~43 mm from anterior pineal foramen to narrowest point). The lateral margins then diverge posteriorly, bounding the posteromedial fossa, and blend into the dorsal surface of the posterolateral rami. The posteromedial fossa is shallow and featureless. On the posterior face, just behind the posteromedial fossa are two parasagittal depressions nearly meeting one another medially, separated by a narrow ridge. The posterolateral rami are relatively short, and horizontally bifurcated distally, to receive the parietal process of the supratemporal. The descending processes are deep and well developed.

Postorbitofrontals — The postorbitofrontals are in articulation with the frontal and parietal. They are well preserved, but there is some dorsal erosion or possible field damage on the dorsal surface of the right one. They broadly underlay the frontal, but significantly less-so, the parietal (Fig. 7). In dorsal view, the element is only visible anterolaterally a short distance before disappearing under the frontal. Examination of the articulation surfaces of the postorbitofrontals and frontal in CT data, indicates the (missing) prefrontal would have contacted the postorbitofrontal, excluding the frontal from the supraorbital margin. Posteromedially, the postorbital meets the parietal in an angular, z-shaped suture, and is inset medially, and thus borders the posterolateral frontal alae posteriorly. The jugal process projects posterolaterally and ventrally, and bears a weak ridge along its anterolateral margin, diminishing anteriorly on the dorsal facing surface of the postorbitofrontal. The distal part of the jugal process is convex anteriorly in cross-section, nearly u-shaped, and slightly curved anteriorly near its distal terminus in lateral view. It is concave posteriorly to receive the dorsal jugal. Ventrally, a strong ridge runs from just medial to the jugal articulation, trending medially, and terminating in an interfingered articulation with the parietal. Posteriorly, the postorbitofrontal gives rise to the blade-like squamosal process. It is thin and dorsoventrally narrow. It appears the squamosal would have articulated with this process far anterior, the sutural contact trending anteroventrally in lateral view.

Squamosal — The right squamosal is preserved and relatively complete, missing a portion of its dorsal process and it is broken and incomplete anteriorly (Fig. 8G-J). The top of the anterolateral wall (lateral ridge of Street and Caldwell, 2016), is relatively straight anteriorly, and at a point parallel to the anterior terminus of the supratemporal articulation on the medial side, forms a crest that slopes posteroventrally, terminating in a sharp point at the convergence of the dorsal, medial, and ventral surfaces. The medial wall is slightly lower than the lateral wall and posteriorly forms the ventral margin of the supratemporal articulation. The articulation for the supratemporal is roughly triangular, its apex directed posteroventrally. In dorsal view, the squamosal bears a deep groove to receive the supratemporal. The quadrate articular facet is well defined and narrow, about one-third the posterior ventral width of the element, and lacks any anteroventral elongation. In dorsal view, the groove to receive the postorbitofrontal is open posteriorly.

Quadrate — The left quadrate of MGUAN PA 183D is complete (Fig. 8A-F) and the right damaged dorsally, missing most of suprastapedial process (Fig. 6A, B). The specimen MGUAN PA 554 (Fig. 10D-J) preserves both quadrates, but they are missing their distal ends, the distal suprastapedial processes, and the alar rims are somewhat weathered, but a segment of the alar groove survives on the left quadrate. Three isolated partial right quadrates were also recovered, MGUAN PA 282 and MGUAN PA 283, missing their distal ends, and MGUAN PA 284, missing the dorsal portion and alar rim.

In lateral view, the suprastapedial extends ventrally to almost mid-height, and nearly touches the quadrate shaft, creating a small auditory meatus, but some of this may be due to taphonomy. The alar cavity (conch) is relatively shallow. The alar groove is deep, and the laterally facing part of the alar rim forms a somewhat wider band of bone posterior to the groove, widening anterodorsally. The posteroventral ascending rim is poorly developed, but steep and blunt. Just medial to the posteroventral ascending rim and just below the suprastapedial process is a well-developed infrastapedial process. Ventrally, the condylar bone is well

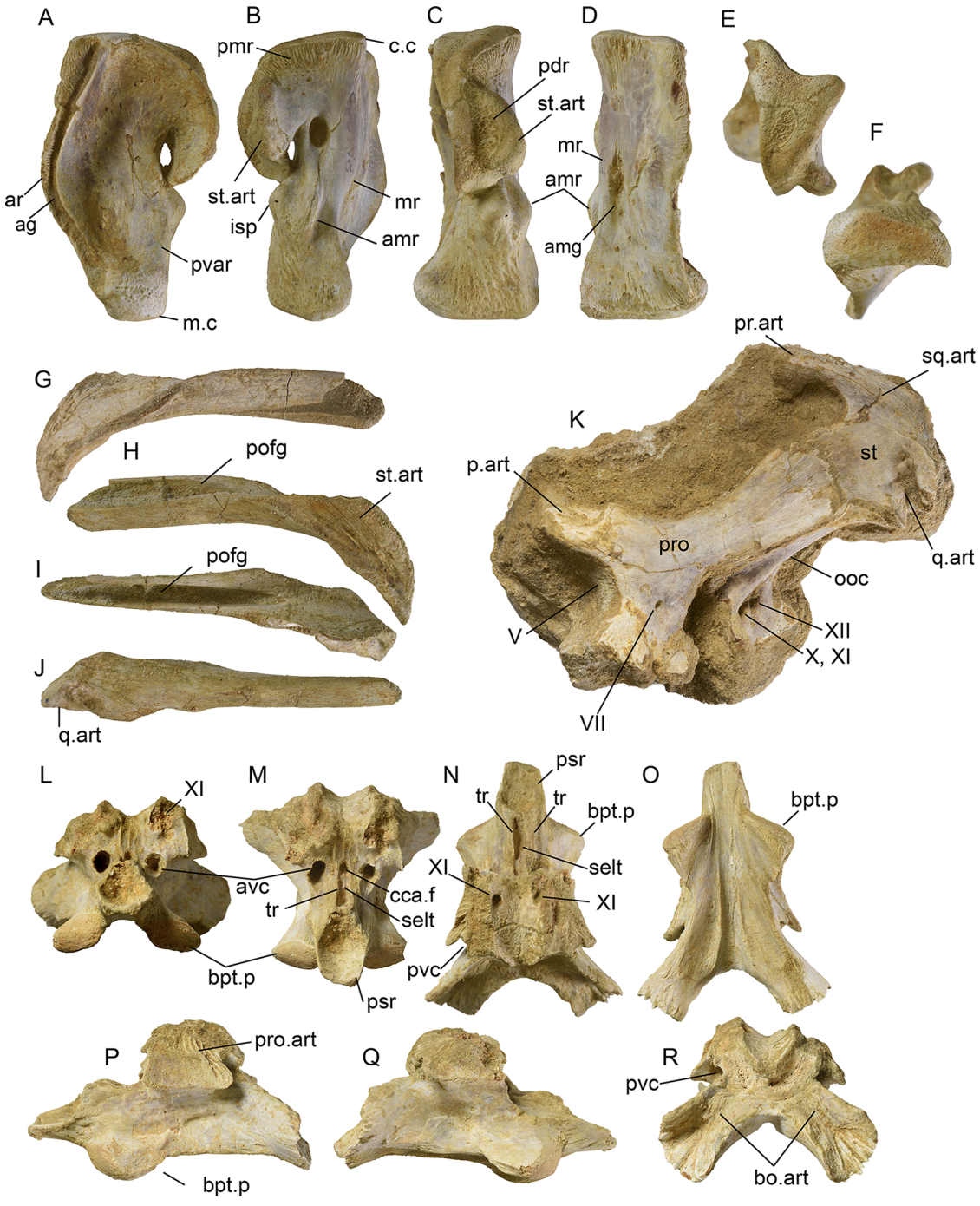

FIGURE 8. Quadrate, suspensorium, and braincase of *Bentiabasaurus jacobsi* gen. et sp. nov. (MGUAN P183D). **A**, left quadrate in lateral view; **B**, same in medial, **C**, posterior, **D**, anterior, **E**, dorsal, and **F**, ventral views; **G**, right squamosal in lateral view; **H**, same in medial, **I**, dorsal, and **J**, ventral views; **K**, articulated left braincase elements in lateral view; **L**, basisphenoid in anterior view; **M**, same in anterodorsal, **N**, dorsal, **O**, ventral, **P**, left lateral, **Q**, right lateral, and **R**, posterior views. **Abbreviations: amg**, anteromedial groove; **amr**, accessory medial ridge; **ar**, alar rim; **avc**, anterior vidian canal; **bpt.p**, pbasipterygoid process; **bo.art**, basioccipital articulation; **cca.f**, foramen for the cerebral carotid artery; **isp**, infraspedial process; **c.c**, cephalic condyle; **m.c**, mandibular condyle; **mr**, medial ridge; **ooc**, otoccipital; **pdr**, posterodorsal rugosity; **pmr**, postermedial rugosity; **pro**, prootic; **pro.art**, prootic articulation; **pvc**, posterior vidian canal; **p.art**, parietal articulation; **pr.art**, parietal ramus articulation; **psr**, parasphenoid rostrum; **pvar**, posteroventral ascending rim; **q.art**, quadrate articulation; **selt**, sella turcica; **st**, supratemporal; **tr**, trabecula; **V**, trigeminal nerve; **VI**, abducens nerve; **VII**, facial nerve; **X**, vagus nerve; **XI**, accessory nerve; **XII**, hypoglossal nerve. Scale bar equals 5 cm.

exposed below the alar cavity, covering the ventrolateral surface.

In medial view the suprastapedial process bears a tall narrow medial boss that inserts in the quadrate articulation of the supratemporal. Anterodorsal to this boss is a depressed area, bearing slight rugosities and well-defined striae dorsally. This area lies adjacent to and largely covers the supratemporal, but does not contact it, suggesting extensive soft tissue between them in life. Ventral to this is the stapedial pit, which is broadly oval, and taller than wide. Just below the stapedial pit, a small ridge rises, extending gradually posteroventrally to a point about one-third the quadrate height terminating just below the level of the infrastapedial process and near the posterior margin of the quadrate shaft. We term this structure the accessory medial ridge. The juncture of the medial surface and the anterior surface forms the medial ridge. This ridge terminates at the cephalic condyle dorsally, below which it becomes increasingly blunt and rounded-over to about mid quadrate height, below which it narrows, its ventral part forming a thin anteromedially directed flange just above the mandibular condyle. Cortical bone covers the ventromedial face of the quadrate shaft to nearly its ventral margin where the cartilage-covered bone of the condyle is minimally exposed.

In posterior view, the suprastapedial process bears an elongate rugose area that separates the supratemporal articulation from the lateral part of the process. The infrastapedial process is visible just below the suprastapedial process, below which the posteroventral face of the quadrate shaft is rugose and weakly striated. The quadrate shaft broadens significantly ventrolaterally and to a lesser degree ventromedially, and the ventral margin formed by the mandibular condyle is flat. Little condylar bone is exposed in posterior view.

In anterior view, the quadrate is tall and laterally narrow, expanding ventrally as described above. On the anterior face is a narrow vertical groove, inset slightly from the medial ridge, its well-defined dorsal terminus slightly above mid-height, and its ventral part forming the apex of a triangular shaped field of bone bounded by the anteriorly expanded alar rim and the medial and ventral margins. We term this "the anteromedial groove".

Braincase

The braincase elements are reasonably well-preserved and only the basioccipital is missing (Figs. 8K-R, 9A-J). The otooccipitals, prootics, and supratemporals are preserved in articulation on both the right and left side, but disarticulated from the basicranial elements and the supraoccipital. The right braincase elements and supraoccipital were left in the block containing the skull roof and partial mandibles (Figs. 6, 7). The left braincase elements and basisphenoid were removed and prepared and scanned separately (Figs. 8, 9).

Prootic — In lateral view (Fig. 9A), the prootic is triradiate, with an anterodorsal process articulating with the supraoccipital and parietal, an inferior process articulating with the basisphenoid and otooccipital, and a posterodorsal process articulating with both the supraoccipital above and the otoccipital medially. The relatively short anterodorsal process bears a deep facet that receives the anteroventral part of the descending process of the parietal, the anterodorsal part of the descending process articulating with the supraoccipital. A large trigeminal notch separates the anterodorsal process from the inferior process. Posterior to the trigeminal notch, the exit for cranial nerve VII is nearly centered on the lateral face of the inferior process, at the dorsal terminus of a sulcus. The ridge forming the anterior margin of the sulcus is homologous with the so-called otosphenoidal crest. The posterodorsal process overlays the otoccipital's posterodorsal process, exposing only the posteroventral part of that element.

Anteromedially, the articulation for the supraoccipital is bipartite, the dorsal portion bearing vertical interdigitating sutures and the ventral part smooth (Fig. 9D). Within the latter, the anterior semicircular canal and the anterior half of the utriculus are visible (Fig. 9E). Slightly anteroventral to the utriculus are the entrances for cranial nerves VII and VIII within a shallow recess. Ventromedially, the inferior process or the prootic articulates with the basisphenoid, bearing vertical interdigitating sutures.

Otoccipital — In lateral view, a portion of the posteroventral part of the otoccipital is visible beneath the prootic ventral margin, its posterodorsal part mostly covered by the supratemporal (Fig. 9A, B). Viewed from behind and left (Fig. 9B, C), an array of external openings is visible. At the anteroventral terminus of a shallow stapedial groove, the round fenestra vestibuli is formed with nearly equal contribution of the prootic. Slightly posterior, the vertically elongate oval fenestra rotunda is separated from the fenestra vestibuli by a narrow crista interfenestralis. On the middle part of the anterior wall of the fenestra rotunda is a foramen for cranial nerve IX. Posteriorly, is a long slit-like foramen which

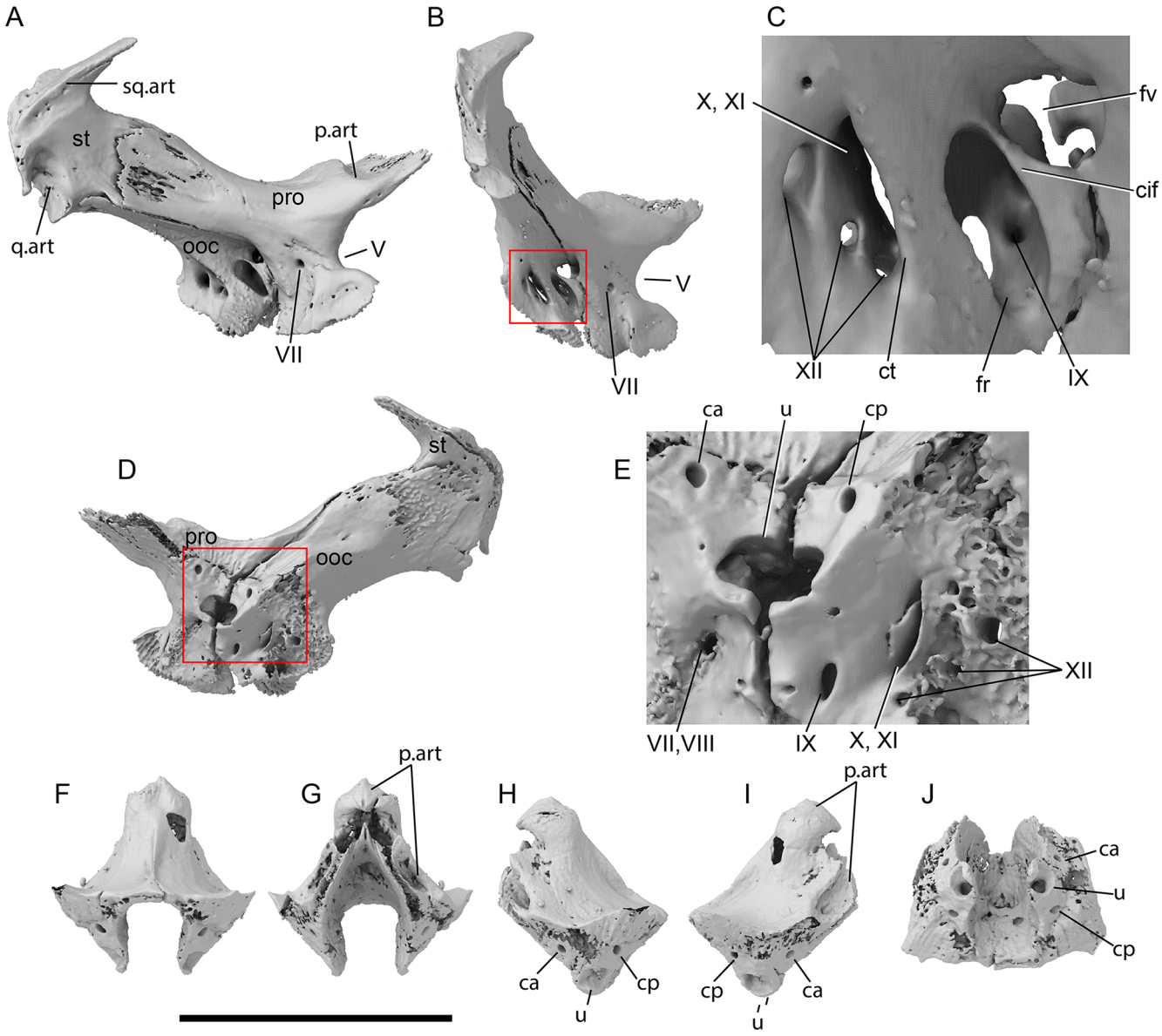

FIGURE 9. Braincase elements of *Bentiabasaurus jacobsi* gen. et sp. nov. (MGUAN PA 183D). **Abbreviations: ca**, anterior vertical semicircular canal; **cif**, crista interfenestralis; **cp**, posterior vertical semicircular canal; **ct**, crista tuberalis; **fr**, fenestra rotunda; **fv**, fenestra vestibuli; **j.f**, jugular foramen; **sq.art**, squamosal articulation; parietal articulation; **q.art**, quadrate articulation; **u**,utriculus; **V**, trigeminal nerve; **VII**, facial nerve; **VIII**, acoustic nerve; **IX**, glossopharyngeal nerve; **X**, vagus nerve; accessory nerve; **XII**, hypoglossal nerve. Scale equals 5 cm.

carried cranial nerves X and XI. This foramen is also thought to have carried the "posterior cerebral branch of the internal jugular vein, and the occipital branch of the internal carotid artery to the lateral surface of the braincase." (Russell, 1967, p. 38). In the posteroventral part of this foramen are two smaller foramina, and a third posterodorsal to those, which carry cranial nerve XII. Posteroventral to these foramina is a small condylar surface (Fig. 8K).

Anteromedially, the otoccipital articulation with the supraoccipital is similar to that described for the prootic, but contributes only about a quarter of the articulating surface area with that element (Fig. 9D, E). The smooth ventral portion preserves the posterior semicircular canal and posterior half of the utriculus. Posteroventrally, the foramen for cranial nerve IX is visible. Posterior to that, is a slit-like foramen carrying cranial verves X and XI, and posterior to

that, the three foramina for cranial nerve XII are present on the broken surface. Posteromedially, the medial surface of the posterodorsal process expands distally, and covers much of the supratemporal (Fig. 9D). The ventral margin curves distally, buttressing the medial part of the quadrate articulation with the supratemporal.

Supratemporal — In lateral view, the supratemporal can be divided into three regions; the articulation for the squamosal dorsally, the articulation for the quadrate medial suprastapedial process ventrally, and between those a large featureless subrectangular area that would have been medial to the dorsal part of the main body of the quadrate in life (Fig. 9A). The squamosal articulation is roughly triangular, a narrow ridge beginning near its posterior apex and trending anterodorsally. This ridge sits within a conjugate groove on the medial surface of the squamosal. The articulation for the quadrate is deep and receives a process on the posteromedial suprastapedial process, separated from the suprastapedial part of the alar rim, by a vertically elongate posterodorsal rugosity. The tight articulation of the supratemporal around this process, rendered the quadrate immobile rostrocaudally, but may have allowed lateral translation of the mandibular joint. In dorsal view, the supratemporal expands anteriorly, articulating with the squamosal posteriorly and the parietal anteriorly.

Basisphenoid — The basisphenoid is relatively complete and well preserved (Fig. 8L-R) with minor only breakage in the anterodorsolateral right part, exposing the path of cranial nerve VI dorsally. Anteriorly the parasphenoid rostrum is a relatively short, shallow u-shaped structure, but may be incomplete anteriorly. The posterior part of the u-shaped rostrum terminates on a posterior wall, with medially sloping lateral margins and a relatively straight dorsal margin, which is the anterior terminus of the sella turcica. The sides of the sella turcica are bound by low thin walls, the trabeculae, which run parallel posteriorly and terminate at the posterior wall, below the dorsum sellae. Slightly above the level of the floor of the sella turcica, on the posterior wall, is a single foramen for the cerebral carotid, which in turn gives rise to the basilar artery. The cerebral carotid branches medially from the internal carotid within the vidian canal. The posterior wall of the sella turcica is vertical and tall, the dorsum sellae slightly concave. The floor of the medullary cavity is nearly perpendicular to the posterior wall of the sella turcica. Lateral to the sella turcica are the anterior openings of the vidian canals anterior to which a shallow sulcus runs anteriorly, lateral to the trabeculae. The posterior opening of the vidian canal is relatively far posterior, but anterior to the basioccipital articulation, hidden below the posteroventral part of the prootic articulation in lateral view (Fig. 8P), but visible in posterior view (Fig. 8R). Dorsal to the anterior opening of the vidian canal is the exit for cranial nerve VI. The entrance for cranial nerve VI is on the lateral margin of the floor of the medullary cavity, one quarter its length posteriorly. The articulation for the basioccipital occupies most of the posterior surface, with long posterolateral processes which would have wrapped around the anterior basal tubers. Anteroventrally, the short subtriangular basipterygoid process, bears an anteroventrally and a slightly laterally directed articular surface (Fig. 8M-Q). In ventral view, there is a ventral median groove whose posterolateral margins are more defined and diverge posteriorly.

Supraoccipital — The supraoccipital is complete (Fig. 9F-J). In posterior view, the supraoccipital is trapezoidal, its sides converging dorsally. Its posterior margin is relatively straight, its medial part forming the top of the foramen magnum. A thin median ridge rises from near the dorsal border of the foramen magnum and trends anterodorsally, and diminishes dorsally. Anterodorsally, the supraoccipital articulated with the parietal in a poorly defined knuckle. Anterolaterally, there are prominent sulci to receive the posterior descending processes of the parietal (Fig. 9G, I). The ventral part forms conjugate articulation with the otoccipital and the prootic, and corresponding openings of the semicircular canals and utriculus.

Pterygoid — The right pterygoid is present but largely obscured, broken, and partially digested. Some tooth bases are visible anteriorly and just anterior to the incomplete ectopterygoid process, set on a high thin ridge, but an accurate count cannot be made. Anteriorly, there is a long thin process visible posterior to which the element widens substantially, together forming the articulation with the palatine. The base of the laterally directed ectopterygoid process anterior margin curves anteromedially, meeting the main body of the pterygoid. The tooth row is taphonomically folded over, almost touching the ectopterygoid process. Posteriorly, in line with the tooth row, there is a broad, transversely concave, quadrate ramus. The basisphenoid process is broken and displaced slightly.

Mandible

The right posterior mandible of MGUAN PA 183D is nearly complete and largely articulated, but the anterodorsal part is broken and slightly displaced along with the coronoid (Figs. 6, 7). The right splenial is closely associated and appears to be in articulation with the prearticular though broken and twisted (Fig. 7B). The left posterior mandible preserves the surangular and angular in close proximity to one another, but the articular is displaced from the bone mass and fragmentary. The left coronoid was also displaced, but well preserved (Fig. 1B). No dentaries are preserved with MGUAN PA 183. Partial dentaries and marginal dentition are preserved in MGUAN PA 554 (Fig. 10). The preserved parts of the quadrates, coronoid, and splenial of this specimen are nearly identical to those in MGUAN PA 183D, and thus confidently identified as *Bentiabasaurus jacobsi* gen. et sp. nov. and used here to describe the dentaries and marginal dentition.

Dentary — The dentaries are badly weathered, fragmentary, and their anterior parts missing (Fig. 10A-C, M, Q, S). There are 11 tooth positions preserved in right dentary and 13 in left, but along with additional isolated and fragmentary alveoli and tooth root parts, the tooth count was at least 15 and possibly higher. The medial parapet is as high as the lateral wall, though it is taphonomically displaced dorsally in the left dentary. In lateral view, the base of attachment is elevated, and in dorsal view, resorption pits are relatively small and visible posteromedial to tooth positions. The posterodorsal edentulous region is about one and a half tooth positions long. The broken tooth bases, the teeth in place, and the isolated teeth are all more or less symmetrically bicarinate, laterally compressed, and slightly recurved posteriorly and medially, and have smooth enamel surfaces (Figs. 10, 11). The teeth vary somewhat in recurvature along the tooth row. The carinae bear no serrations.

Splenial — The right splenial is nearly complete in MGUAN PA 183D, but the anterior part is broken and rotated out of position (Figs. 7B, 12A-D). A fragmentary right splenial is preserved in MGUAN PA 554 (Fig. 10K, L). In dorsal view, the body of the splenial gives rise to a short lateral and a taller medial dorsal lamina that would have received the prearticular between them posteriorly. There are two small foramina in the posterior floor, anterior to which the internal opening of the large anterior mylohyoid foramen is visible piercing the medial wall. In lateral view the posterior border is gently arcuate, the dorsal part extending slightly more posterior than the ventral (Fig. 12B). The dorsal and ventral margins are nearly parallel posteriorly, and the dorsal margin quickly slopes anteriorly beginning at the level of the anterior mylohyoid foramen, and is narrow anteriorly. In medial view, the posterior margin is embayed at about mid-height (Figs. 10K, 12D), the dorsal and ventral parts extending posterior about equally. The medial lamina rises near the posterior margin, sloping gradually antero-dorsally reaching its apex at about one-third the preserved length of the splenial. The emargination for the anterior inferior alveolar foramen is visible on the dorsal margin between the anterior margin of the anterior mylohyoid foramen and the apex. Anterior to the apex, the dorsal margin slopes gradually anteroventrally, the anterior two-thirds of the preserved splenial forming a roughly triangular shape. In posterior view the central part of the splenial is shallowly recessed, the dorsomedial part more recessed and meeting the dorsal surface of the splenial (Fig. 12C).

Angular — The right and left angulars are preserved in MGUAN PA 183D, the right still in articulation with the surangular and articular (Figs. 7, 12E-J). It is relatively narrow in anterior view, the anterior medial flange extending more anterior than the lateral, and forming a shallow dorsal triangular depression between them. In medial view, the posterior margin is only slightly posterodorsally oriented and slightly concave (Fig. 12H). In lateral view, the posterior margin rises at a shallow angle posterodorsally, then turns posterior at the suture with the surangular, narrowing slightly posteriorly (Fig. 12F, I). The posterior mylohyoid foramen is obscured, but can be seen in cutaway views (Figs. G-G_2) relatively low on the medial side. The posterior part is not visible.

Surangular-Articular — The right surangular and articular are broken, but largely in articulation in MGUAN PA 183D (Figs. 6, 7). In lateral view, the anterior part of the surangular is narrow, its ventral margin sloping posteroventrally at a shallow angle to meet the angular at a point below the middle of the coronoid facet. The anterior surangular foramen lies relatively far posteriorly, dorsal to a point near the anterior terminus of the angular. The coronoid articulation is long and buttressed posteriorly by the anterodorsal sloping dorsal margin of the surangular that rapidly rises just anterior to the glenoid. The glenoid is formed about equally by the articular and surangular and bears a prominent anteromedial foramen.

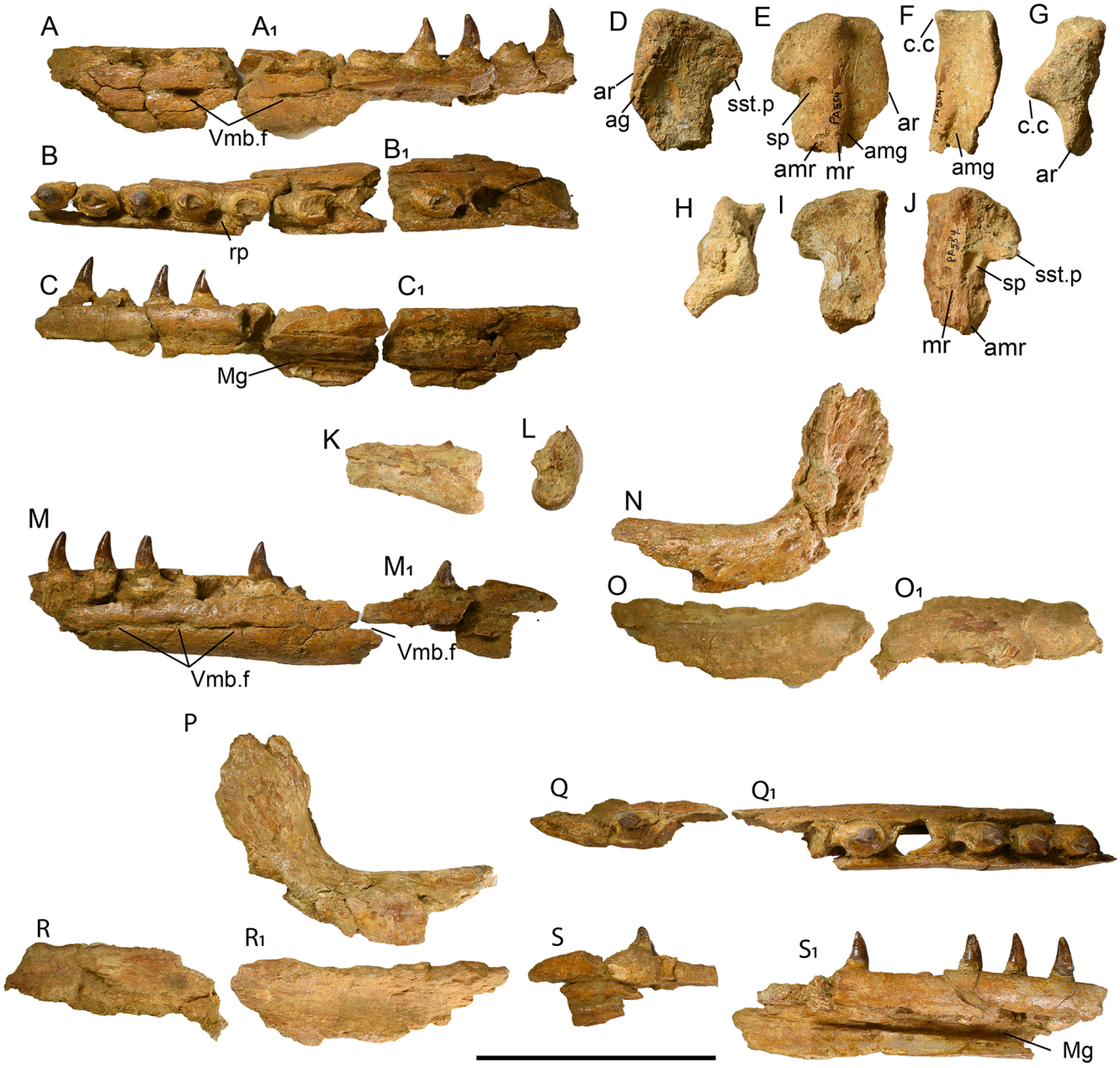

FIGURE 10. *Bentiabasaurus jacobsi* gen. et sp. nov. (MGUAN PA 554) partial mandibles and quadrates. **A**, posterior partial right dentary in lateral, **B**, dorsal, and **C**, medial views; **D**, left quadrate in lateral, **E**, medial, **F**, anterior, and **G**, dorsal view; **H**, right quadrate in dorsal, **I**, lateral, and **J**, medial views; **K**, posterior fragment of right splenial in medial, and **L**, posterior views; **M**, posterior partial left dentary in lateral, **Q**, dorsal, and **S**, medial views. **N**, left coronoid in lateral, and **P**, medial views. **O**, fragmentary left surangular in lateral and **R**, medial views. **Abbreviations: ar**, alar rim; **ag**, alar groove; **amg**, anteromedial groove; **amr**, accessory medial ridge; **c.c**, cephalic condyle; **lc**, left coronoid; **ldent**, left dentary **lq**, left quadrate; **lsur**, left surangular; **Mg**, Meckelian groove; **mr**, medial ridge; **rp**, resorption pit; **rs**, right splenial; **rt**, replacement tooth; **rq**, right quadrate; **sp**, stapedial pit; **sst.p**, suprastapedial process; **Vmb.f**, foramen for mandibular branch of trigeminal nerve. Scale bars equals 5 cm.

In lateral view, the surangular-articular suture begins at the posterior glenoid, then slopes posteroventrally a short distance, then turns and slopes gently anteroventrally. The retroarticular is broadly trapezoidal and projects posteriorly without significant medial deflection. In medial view, near the center of the retroarticular, is a single small foramen for the chorda

FIGURE 11. *Bentiabasaurus jacobsi* gen. et sp. nov. (MGUAN PA 554) marginal dentition. **A**, anterior portion of preserved posterior right dentary in dorsal view; **B**, fragment of left dentary in dorsal view; **C**, anterior portion of preserved posterior left dentary in dorsal view. **D**, disarticulated, associated marginal tooth in medial, **E**, lateral, **F**, posterior, **G**, anterior, and occlusal **H**, views; a second disarticulated, associated marginal tooth crown in medial, **E**, lateral, **F**, anterior, **G**, posterior, and occlusal **H**, views; **I**, left dentary fragment in posterolateral view. **Abbreviations: rp**, resorption pit; **rt**, replacement tooth. Scale bars equal 5 cm.

tympani. The surangular-articular suture begins at the antero-medial part of the glenoid, and slopes gently anteroventrally and then horizontally more anteriorly, medial to which is a large mandibular fossa.

Coronoid — Both coronoids are present with MGUAN PA 183D (Fig. 7) and the left is preserved with MGUAN PA 554 (Fig. 10N, P). In lateral view, the lateral face of the coronoid is arcuate, the horizontal ramus longer than the vertical, the two rami diverging at about 115°. The anterior end of the lateral face is pointed, the dorsal and ventral margins diverging gently posteriorly, then turning postero-dorsally and narrowing again, converging and meeting posterodorsally in a

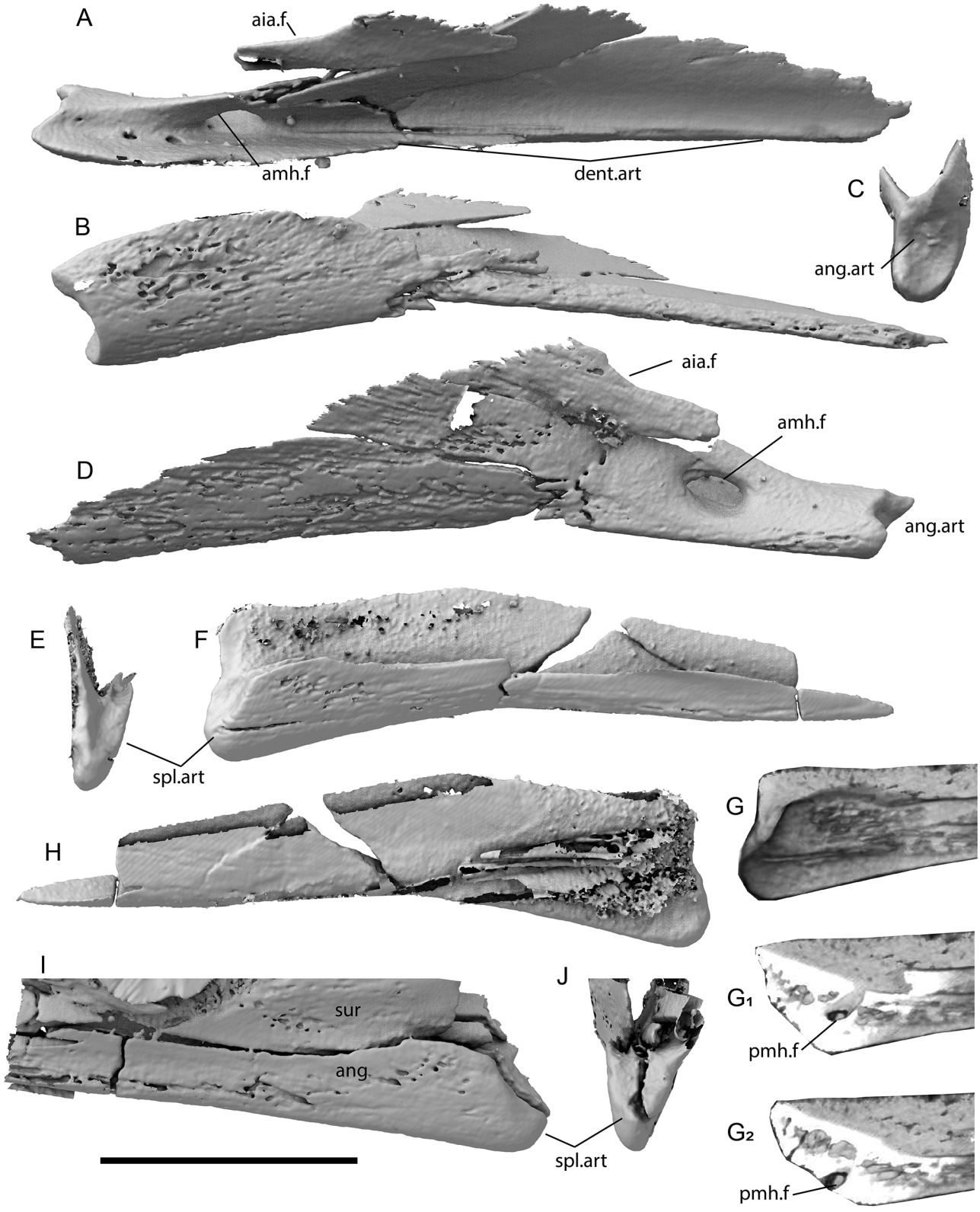

FIGURE 12. Splenial and angular of *Bentiabasaurus jacobsi* gen. et sp. nov. (MGUAN PA 183D). Right splenial in **A**, dorsal, **B**, lateral, **C**, posterior, and **D**, medial views; **Abbreviations: aia.f,** margin of anterior inferior alveolar foramen; **amh.m**, anterior mylohyoid foramen; **ang**, angular; **ang.art**, angular articulation; **dent.art**, dentary articulation; **pmh.f**, posterior mylohyoid foramen; **spl.art**, splenial articulation; **sur**, surangular. Scale equals 3 cm.

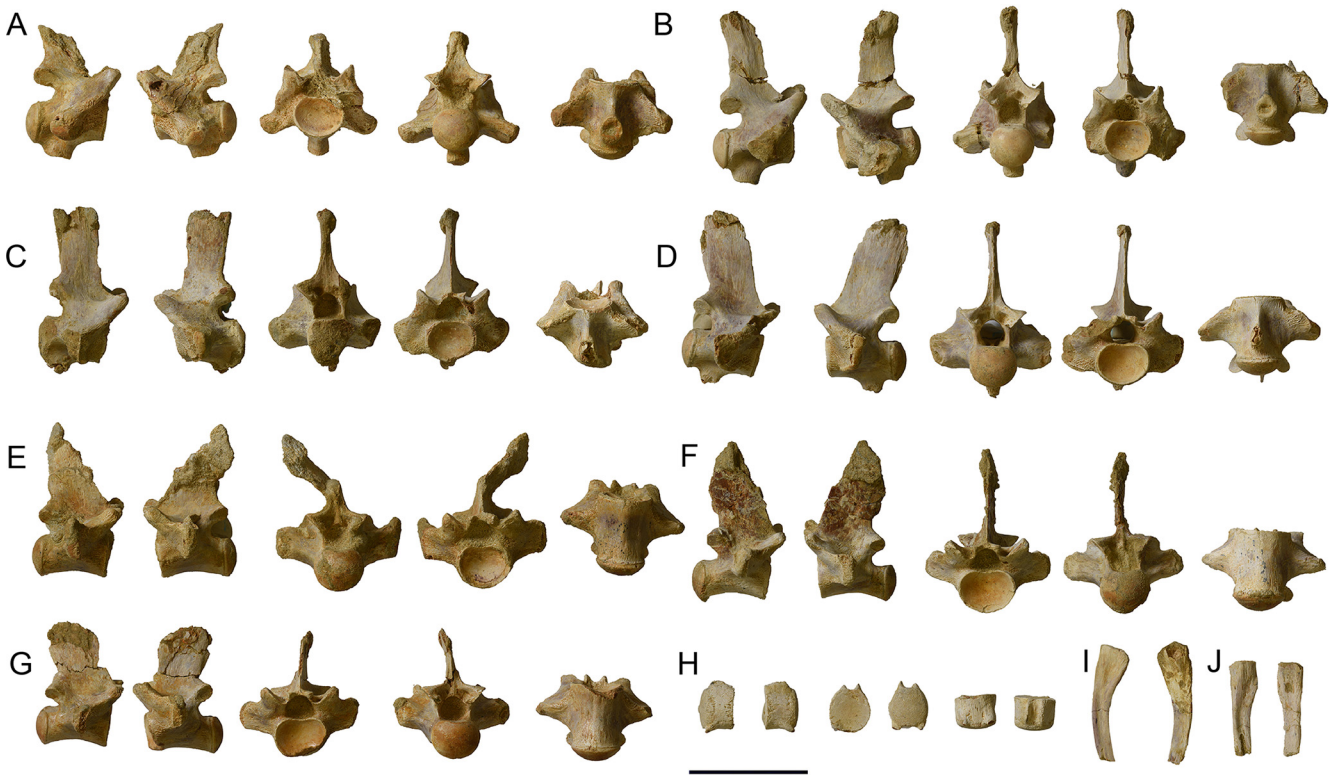

FIGURE 13. Representative vertebrae of *Bentiabasaurus jacobsi* gen. et sp. nov. (MGUAN PA 183D). **A**, cervical vertebra three; **B**, cervical vertebra five; **C**, cervical vertebra six; **D**, cervical vertebra seven; **E-G**, thoracic trunk vertebrae; **H**, terminal caudal vertebra; **I**, **J**, cervical ribs. All vertebrae arranged from left to right in right lateral, left lateral, anterior, posterior, and ventral views. Scale equals 5 cm.

point. In lateral view, the medial face of the posteromedial process is visible, and bears a large contact area where it would have been overlain by the anterior part of the surangular buttress. The posteroventral vertical ramus bears a deep groove for insertion of the adductor musculature. In medial view, the medial ventral margin is only slight deeper than the lateral and would not meet the angular. The posterior margin of the medial ventral flange is notched, posterior to which the coronoid medial face broadens posteriorly, its posteroventral part overlapping the medial surangular and its dorsal part bearing striations. In dorsal view, there is no evidence of an anterior cleft.

Postcrania

Cervical vertebrae — There are four cervical vertebrae preserved with MGUAN PA 183D (Fig. 13A-D), which we interpret as representing positions C3, and C5-C7 based on development of synapophyses and hypapophyseal peduncles. No hypapophyses are preserved. Articular surfaces are nearly circular, with some dorsal emargination below the neural canal anteriorly and slightly progressively more depressed posteriorly. The dorsolateral trending contact of the zygopophyses is about 45 degrees. Though missing due to breakage C3 and C5, well-developed zygosphenes and zygantra are present on others. The rib facet on C3 is small and slightly oval, becoming more vertically elongate posteriorly. C3, and C5 bear well preserved peduncles, broken in C6, and C7 does not bear an articular facet for the hypapophysis. The anterior margin of the peduncles is drawn out anteriorly, making the articular surface weakly teardrop shaped. None of the neural spines are complete, but the above the level of the postzygapophyses, C3 is posteriorly broad, forming a somewhat triangular cross-section, the posterior width diminishing in more posterior vertebrae. Anteriorly the preserved parts of the neural spines are narrower in lateral view, and become broader in the more posterior ones.

Trunk vertebrae — There are six trunk vertebrae and three of those free of matrix and well preserved enough for description and interpreted as coming from the thoracic region based on their relatively deep synapophyses (Fig. 13E-

G). The articular surfaces are nearly circular, but appear more depressed than the cervicals, due to increased flattening of the dorsal rim, beneath the neural canal. The dorsolaterally trending contact of the zygopophyses is about 45°. All elements in which the area is preserved bear well-developed zygosphenes and zygantra. Although they are broken distally, the preserved parts of the neural spines are similar to C7, broad and trending posterodorsally.

Caudal vertebrae — There are five caudal vertebrae, only two of which are free of matrix and of those, one well preserved well-enough to be described (Fig. 13H). It is partially digested, the neural and hemal spines reduced to their bases, and the cortical bone partially decalcified. It is identified as a terminal caudal by lack of transverses processes on its lateral sides. The articular surfaces are slightly taller than wide (1.07:1), the ventral part is arcuate, forming a semicircle, and the dorsolateral margins slightly flatter and converge with the dorsal margin which is embayed beneath the neural canal. The articular surfaces are only minimally curved. The centrum is relatively short compared to its articular height (0.64:1).

DISCUSSION

The remarkable specimens reported here provide a unique snapshot of ancient trophic interactions that took place in a highly productive upwelling zone along the west coast of Africa approximately 71.5 Mya. The fossil reveals aspects of the feeding behavior of *Prognathodon kianda* including prey selection, acquisition, processing, and digestive biology. Furthermore, the fossil provides an empirical basis to discuss the relationship of tooth morphology and prey processing, and also allows comparison with other putative gut-content occurrences. In the following paragraphs, we provide additional context for the locality and the range of trophic interactions preserved there. We then discuss size relationships of the predator and prey items, prey completeness and prey processing.

The "Bench 19 Bonebed" — The fossils described herein were collected from a horizon that preserves an extra-ordinarily dense concentration of marine amniote fossils, referred to as the "Bench 19 Bonebed" located at Bentiaba, Namibe Province, Angola (Strganac et al., 2015a). The bonebed is restricted to outcrops in erosional channels and hillsides, all within a very small area (100,000 m^2) and a stratigraphically restricted horizon (~10 m). The greatest concentration of bone falls within the first few meters above Bench 19, the topmost of a series of resistant sandstone benches exposed on the sea cliffs adjacent to the site. The bonebed preserves two plesiosaur taxa, four turtle taxa, and at least seven mosasaur taxa (Strganac et al., 2015a). There are also numerous fishes, pterosaurs, and occasionally dinosaurian elements found. The density of preserved vertebrate marine life has been explained as the result of attritional accumulation in a highly productive upwelling area (Jacobs et al, 2009), occurring within a relatively short time-frame (240 kyr) falling within magnetochron 32n.1n, and dated at 71.40-71.64 Ma (Strganac et al., 2014; Jacobs et al., 2016). The continental shelf is quite narrow along that part of the coast and together with the sedimentology at the site indicates the locality of Bentiaba was deposited in a relatively nearshore, cold water paleoenvironment (Strganac et al., 2015a; 2015b).

Paleo-foraging-area — Strganac et al. (2015a) inferred foraging area preferences for select marine amniotes in the Bench 19 fauna at Bentiaba using stable carbon isotopes. Of those taxa analyzed, two of them (*Halisaurus* and *Gavialimimus*) were found to exclusively occupy the nearshore foraging area (about −7 $\delta^{13}C$), while a third (*Prognathodon kianda)* occupied the widest range of foraging areas, including the nearshore (−7 to −15 $\delta^{13}C$). *Bentiabasaurus jacobsi* was not included in that analysis; however, large *Mosasaurus* cf. *M. hoffmanni*, were included and were found to occupy an offshore foraging area (−10 to −13 $\delta^{13}C$), consistent with the absence of body fossils of that taxon at the locality, known only from a few isolated shed teeth, suggesting it only occasionally visited the nearshore environment. The taxa *Gavialimimus* sp. and *Prognathodon kianda* found in the gut of MGUAN PA 183, along with those taxa plus parts of multiple individuals of *Halisaurus* sp. in MGUAN PA 25, the isolated regurgitalith reported in Strganac et al (2015a), and *Bentiabasaurus jacobsi* are all represented by body fossils at the locality. Thus, it is likely that all of the prey items and their predator died and were preserved were they foraged.

Trophic interactions — Although shark scavenging on the marine amniote skeletons is common at the locality (Fig. 2), the only evidence of trophic interactions among the marine amniotes are the remains of the *Prognathodon kianda* (MGUAN PA 183) and its associated gut-content described herein and one other bone mass, interpreted as a regurgitalith (MGUAN PA 25), and briefly mentioned by Strganac et al.

(2015a). The latter is undergoing preparation and will be addressed in detail elsewhere, but also contains the remains of *Gavialimimus* sp., *Prognathodon kianda,* and *Halisaurus* sp. The size of the regurgitalith would have been impossible to pass through the small gape presented by the elasmosaurid plesiosaurs known from the site. A large offshore foraging predator like *Mosasaurus* cf. *M. hoffmanni,* known to be transient at the locality, may have been the maker of the regurgitalith. However, given that the size, taxonomic composition, and morphology of the regurgitalith is quite similar to that seen in MGUAN PA 183, and *P. kianda* is the most common large predator preserved at the site, it is most likely attributed to *P. kianda*. There is no evidence of predation by mosasaurs on any of the plesiosaur material recovered.

The predator — *Prognathodon kianda* (MGUAN PA 183) has a reconstructed skull length of about 713 mm measured at the midline and a snout-vent length of about 3.64 m approximating the vent at the start of the caudal series. Head to body length proportions for select mosasaur taxa and estimated lengths for others was provided by Russell (1967, p. 208-210) and using the skull measurements of the predator, we estimate the animal was about 6.5-7 meters long in life. In PA 183 some of the anterior teeth are broken and missing but there is no sign of apical wear on those that remain. More posterior well-preserved teeth present in the maxillae (position 7+) and dentaries (position 8+), show no signs of apical wear (Fig. 2A). The first tooth in the right dentary and corresponding premaxillary tooth do show conjugate tooth-on-tooth wear anterolateral on the dentary tooth and posteromedially on the premaxillary tooth. Anterior teeth are nearly circular at their bases and with a high base to length aspect ratio in the first few positions, but become increasingly laterally compressed posteriorly. All marginal teeth are bicarinate, with slightly greater contribution of the lingual surface, and posteriorly carinae are sharp and well developed, and the crowns slightly recurved posteriorly. These posterior teeth fall within the "cut guild" of Massare (1987), for which she predicts prey items to include large fish and reptiles. They are also consistent with the "flesh cutter guild" of Fischer et al. (2022). However, *Prognathodon kianda*, like many members of globidensini, possesses a highly heterodont tooth row. The anterior teeth in *P. kianda* are prognathous and conical, seemingly better suited for gripping or manipulating prey than cutting flesh. Additionally, and as with many globidensins, *P. kianda* possesses a tall anterior premaxilla in the part of the tooth row containing the prognathous dentition. The beam strength of a given thickness of bone increases at the square of its height, suggesting the anterior part of the snout in this group may have been adapted to dealing with higher compressional stresses in the sagittal plane than those taxa in the narrower low-snouted Plotosaurini. In any event, the more posterior teeth were clearly suited to "flesh cutting" and together with the anterior teeth, and large recurved pterygoid teeth (Schulp et al., 2008), were likely used in a repertoire of actions for prey prehension, processing, and ingestion.

Preservation and taphonomy of prey items — Differences in tissue cover, and the degree of articulation at time of ingestion and throughout digestion, are reflected in the relative decalcification and erosion of bone surfaces. Differential digestion likely indicates durability and/or thickness of soft tissue covering. For instance, the inferred attachment area for temporal musculature of the parietal is pristine, and bone surfaces on the pterygoid and posterior mandible which would have anchored large muscle masses such as the pterygoideus are also well preserved. Conversely, areas directly exposed to stomach acids such as tooth crowns are nearly completely eroded. Those areas with presumably thin soft tissue cover, such as the snout and skull roof are significantly decalcified.

There are also some differences in preservation of those elements in the hindgut versus those in the foregut. Some of the best-preserved elements are present in the foregut region, near the back of the skull of MGUAN PA 183D (Figs. 8, 9). These elements show little or no erosion, suggesting they had not been subjected to the full strength of and/or long exposure to the stomach acids, compared to those elements in the hindgut. Contrast this with the preservation of MGUAN PA 183B, in which large portions of the dentary and quadrate have been digested. No tooth crowns are present, including replacement teeth, though anterior portions of the snout of MGUAN PA 183D found in the hindgut do preserve replacement teeth, but as noted above, these elements may have been transported. Nonetheless, even in the hindgut, durability of the soft tissue appears to have protected large parts of the braincase and pterygoids.

The degree of digestion in the stomach content of MGUAN PA 183 is generally greater than seen in the examples presented by Longrich et al. (2022). In those, eroded teeth

ranging from slight enamel damage to complete erosion of the crown are present. However, the erosion of the bone surfaces in those same specimens does not appear to be as great. These differences between the Moroccan and Angolan samples may simply be due the amount of time the food parcel was in the stomach prior to egestion. In the case of MGUAN PA 183, there is differential erosion of elements found in the hindgut compared to the foregut, demonstrating at least a qualitative difference is degree of digestion due to resident time. It may also indicate taxonomic differences in digestive biology or possibly differences in digestion efficiency as a function of temperature. Mosasaurs did have high metabolic rates, with estimated body temperatures ranging from ~35° to ~39° reported by Bernard et al. (2010) and ~33°C to ~36°C reported by Harrell et al. (2016), or between ~2°C and ~8°C above ambient sea temperature. However, mosasaurs may not have been homeothermic, their body temperature influenced by ambient temperature (Bernard et al., 2010). In the case of the Moroccan sample, sea surface waters were relatively warm in the Maastrichtian, approximately 27°C (Lécuyer et al., 1993) compared to Bentiaba which was about 18°C (Strganac et al., 2015a). If body temperature does covary with sea temperatures, and digestive efficiency is a function of temperature, this may account for some differences in the level of decalcification seen in the two samples.

Estimated size of prey items — In the case of the fossils here, all of the inferred food parcels are of a relatively small size and include discontinuous portions of the prey items body in some cases, suggesting some level of dismemberment prior to ingestion. With few exceptions, most individual bones appear to have been complete at the time of ingestion, and do not show any apparent trauma, including longer dentigerous elements. Intuitively, physical constraints, such as the size and elasticity of the esophagus would be a major factor in limiting the maximum prey parcel size that could be ingested.

The length of preserved dentary preserved with *Gavialimimus* sp. (MGUAN PA 183B) is ~375 mm long, and is the longest individual element among the gut-content. The articulated braincase preserved with that specimen, if uncrushed, is estimated to have had a minimum diameter of ~200 mm at the time of ingestion, and is the largest diameter parcel taken. Scaled to the dentary, the skull would have been an estimated at 532 mm in length at midline. Although *Gavialimimus* sp. is a plioplatecarpine, it has an unusually long and narrow skull (Strong et al., 2020), and the measurements and estimates given by Russell (1967, p. 208-210) are for short faced plioplatecarpines such as *Platecarpus* and *Plioplatecarpus*. We therefore instead use an average of his estimates for the elongate skulled *Tylosaurus,* yielding a total body length of about 4 meters, or approximately 57% the body length of the predator.

Judging by the lack of decalcification of the internal surfaces, the isolated snout elements of *Prognathodon kianda* (MGUAN PA 183C) were likely in articulation at the time of ingestion. There are no prefrontals or palatal elements recovered, and there is no evidence of truncation; however, the most posterior parts of both maxillae were not recovered. The articulated snout would have had a maximum posterior diameter of about ~100 mm and a length of ~220 mm. Comparing the size of the snout with more complete specimens, the skull is estimated to be ~470 mm midline length and would have had a maximum diameter of ~285 mm. Again, using the methods of Russell (1967, p. 208-210) the animal is estimated to have been about 4.6 m total length, or approximately 66% the size of the predator.

The most complete and smallest specimen is *Bentiabasaurus jacobsi* gen. et sp. nov. (MGUAN PA 183D). The mandible length is estimated to be ~400 mm and the skull ~365 mm midline length. The skull and mandibles, if articulated when consumed, would have measured ~150 mm maximum diameter and ~400 mm in length, and would have represented the largest single food parcel volumetrically. Given that this appears to be a gracile form, the body length was estimated using the data give by Russell (1967) for *Clidastes liodontus*, in which the head is 12.1% of total body length. This would suggest MGUAN PA 183D would have been just over three meters in length. However, if we use the proportions given by Russell (1967) on *Mosasaurus hoffmanni* it could have been as long as 3.7 meters. This gives a range of between 47-53% the body length of the predator.

Fischer et al. (2022) used interglenoid distance as an estimate of gullet diameter, and thus the limiting factor for ingestion of food parcels. The reconstructed interglenoid distance in MGUAN PA 183 is ~270 mm. Given the largest food parcel diameter noted above was the braincase of the *Gavialimimus* sp. at about 200 mm, there would be no issue with ingestion even with other elements such as the pterygoids and mandibular parts adherent. However, an articulated and uncrushed skull and mandibles of a *Gavialimimus* scaled to the size of the dentary present, would approach the upper

limits of what the gullet could pass. The maximum diameter of an uncrushed and articulated skull of *Prognathodon,* scaled to the preserved snout, would have been ~285 mm and thus would have exceeded the diameter of the gullet. So, in the case of the *Gavialimimus* and *Prognathodon* skull parts, some level of dismemberment was required, at least for a predator the size of MGAUN PA 183, while a smaller complete skull and mandibles such as those of *Bentiabasaurus jacobsi* gen. et sp. nov. would not.

All of the prey items were considerably smaller than the predator in life, ranging from 43-57% the body length of the predator. In an analysis of prey size taken by marine predators, Costa (2014) found "that larger predators increase the maximum size of the prey that they consume while also increasing minimum prey size". In the case presented here, the predator appears to be taking prey sizes up to the limits of its ability to pass through its gullet, but no smaller prey items have been identified. That is also the case with the undescribed regurgitalith (MGUN PA 25). This may be an artifact of the availability of large prey items in this rich ecosystem, maximizing calorie intake for a given feeding bout.

A cannibal headhunter? — Curiously, most of the prey items in the stomach of MGUAN PA 183 are cranial elements. Two of the prey species likely carried with them all or parts of the adductor mandibulae and the pterygoideus. These large muscles would of course provide some needed calories, but the cost of acquisition seems inefficient for an active predator, raising the possibility these are scavenged meals. The paleoproductivity evident at the locality in the form of the dense concentration of marine amniote carcasses supports this speculation, providing ample opportunity for free or cheap meals. Additionally, the second regurgitalith reported by Strganac et al. (2015a) does contain a substantial number of vertebrae of a small halisaurine taxon along with the skull parts of at least three individuals of this taxon. However, no ribs or limbs are present, suggesting these elements were removed by others predators and/or scavengers prior to being eaten by the regurgitalith maker. It would not appear that *Prognathodon kianda* was an obligate scavenger given its morphology, and was more likely an opportunist, and like many carnivorous animals, taking a free meal when available and hunting when necessary.

Though unusual, this is not the first report of headhunting nor cannibalism in the fossil record, both being reported in a semi-aquatic reptile from the lower cretaceous of China (Wang et al., 2005). In that case, seven skulls of juvenile *Monjurosuchus splendens* were found in the abdominal cavity of an adult of the species. In fact, it appears that cannibalism is relatively common in extant reptiles (Mitchell, 1986), and although the data presented terse, it appears it is not uncommon for juveniles and subadults to be preyed upon, at least occasionally, by conspecific adults. This is also supported by data-oriented surveys, such as that of Mateo and Pleguezuelos (2015) that accessed the prevalence of cannibalism through collection and analysis of a large number of fecal pellets of the lacertid *Gallotia caesaris*. The diet of *Gallotia* is mainly herbivorous, secondarily insectivorous, and vertebrates constitute a minor component. In that taxon they found only males preyed on conspecifics, in line with their sexually dimorphic large size, and cannibalism was seasonally linked to the species reproduction cycle, yielding young prey availability during the summer and fall. Nonetheless, cannibalism was only detected in about 0.7% of the 11,651 fecal pellets examined, suggesting overall, cannibalism is relatively rare in this species. Cannibalism has also previously been reported in primarily carnivorous monitor lizards (Shine et al., 1996; King and King, 2004; Stanner, 2004; Géczy, 2009) but those instances are isolated captive or field observations, so it is unclear how common this behavior is in natural populations.

Comparisons with other reports — There are few examples of mosasaur gut-content and those containing other mosasaurs are even more rare. The only published, peer reviewed reports of mosasaur-on-mosasaur predation are those of Martin and Bjork (1987) and Strganac et al. (2015a) while others remain undescribed (Anonymous, 1962; Bell and Barnes, 2007). The report by Martin and Bjork (1987) was "a mat of bones that is partially mixed yet retains some order", which we assume meant the remains were somewhat taxonomically segregated like that described herein. However, unlike our specimen, the mass reported by Martin and Bjork (1987) was a mix of fish, bird, and mosasaur remains, and was found in the pelvic and prepelvic region of the body, presumably near the cloaca, and had therefore presumably passed through the intestines. This is similar to the position of the gut-content preserved with a specimen of *Prognathodon overtoni* (Konishi et al., 2011), which is also located in the hind quarters near the pelvis. In the latter case, the vertebrate gut-content included turtle and fish remains.

Mosasaur-on-mosasaur predation has also been inferred

from disgorged regurgitaliths (Strganac et al., 2015a; Longrich et al., 2022). In both cases, the modifications to remains are nearly identical to that seen in the gut-content MGUAN PA183. Both possess similar patterns of tooth crown erosion, bone decalcification, the presence of anatomical associations, and similar patterns of parcel size, and dismemberment. Comparison with the in-situ preservation reported here, it is reasonable to interpret those reported by Longrich et al. (2022) as regurgitaliths. However, their attribution to *Thalassotitan atrox* may not be warranted as other large mosasaurid predators are also present in the fauna (Bardet et al., 2015). Interestingly, the regurgitalith examples given by Longrich et al. (2022) are mostly portions of mosasaurid skulls and mandibles, but some also contains turtle and fish material as well, whereas the example of Strganac et al. (2015a) also includes significant postcranial elements of one of the preserved taxa and is exclusively mosasaurids. In any event, the preservation of in-situ gut content as reported here, the cololites reported by (Martin and Bjork, 1987; Konishi et al., 2011), and the regurgitaliths reports (Strganac et al., 2015a; Longrich et al., 2022), suggests digestive biology and methods of elimination in mosasaurs was diverse.

CONCLUSION

We reported here a semiarticulated specimen of *Prognathodon kianda* containing well-preserved in situ-gut-content from the "Bench 19 Bonebed" locality at Bentiaba, Angola. We described the preservation and morphology of the gut content and assigned it to three different mosasaurid species including *Gavialimimus* sp., *Prognathodon kianda*, and a new mosasaurine taxon *Bentiabasaurus jacobsi* gen. et sp. nov. The new taxon is related to *Mosasaurus* and *Plotosaurus* but retains a mosaic of plesiomorphic and derived characters. The diversity present in the gut-content represents taxa consumed in their preferred foraging area as evidenced by stable carbon isotopes. The presence of a subadult *Prognathodon kianda* in the stomach of a mature individual of the same species represents the first documented case of cannibalism in mosasaurs. Trophic interactions at the "Bench 19 Bonebed" locality appear to be controlled in part by relative size, with all prey taxa at roughly half of the predator's body length and food parcels approaching the estimated maximum sizes that can pass the gullet. Prey items were all apparently reduced in size through dismemberment prior to ingestion of individual parcels, though details of that process are unknown. Though the sample is quite small, the observed range of modalities suggests prey processing, digestive biology, and methods of elimination in mosasaurs was diverse.

ACKNOWLEDGMENTS

We are thankful to the organizers of this Festschrift for allowing us to honor our friend and colleague Louis L. Jacobs with this contribution. His career has taken him around the world, to all continents, exploring many periods of Earth history and numerous taxonomic groups. We, as members of Projecto PaleoAngola, are thankful for being a part of one leg of his journey. Our work in Angola has been supported by National Geographic, the Petroleum Research Fund of the American Chemical Society, LS filmes, Luanda, Angola, the Dutch Embassy in Angola, ISEM at SMU, and many friends and colleagues in Angola, and we are thankful to all of them. We thank the dozens of SMU students that helped with the conservation of MGUAN PA183 and its final meals. We thank the volunteers, staff, and SMU alumni that helped with preparation including Tyler Nelson, Connor Flynn, Rocky Manning, and Larry Bell. Diana Vineyard, Wayne Furstenwerth, and Bill Stenberg. We are especially indebted to Bill Johnson, who saw the project through from opening of field jacket number one to helping build the mounts and reproductions of the specimens for public display. Finally, we thank Nick Longrich and Amelia Zietlow for their constructive reviews of the manuscript.

AUTHOR CONTRIBUTIONS

MJP and AAS designed the project, OG facilitated field work and project logistics in Angola, MJP drafted the manuscript and figures, MJP and AAS analyzed the data and all authors contributed to refining and editing the manuscript.

LITERATURE CITED

Anonymous. 1962. Reptiles of Saskatchewan's ancient seas. *Saskatchewan Museum of Natural History, popular series* 1, 12 pp.

Araújo, R., Polcyn, M. J., Schulp, A. S., Mateus, O., Jacobs, L. L., Gonçalves, A. O., & Morais, M.-L. (2015a). A new elasmosaurid from the early Maastrichtian of Angola and the implications of girdle morphology on swimming style in plesiosaurs. *Netherlands Journal of Geosciences – Geologie en Mijnbouw*, 94, 109–120. https://doi.org/10.1017/njg.2014.44

Araújo, R., Polcyn, M. J., Lindgren, J., Jacobs, L. L., Schulp, A. S., Mateus, O., Gonçalves, A. O., & Morais, M.-L. (2015b). New aristonectine elasmosaurid plesiosaur specimens from the Lower Maastrichtian of Angola and comments on paedomorphism in plesiosaurs. *Netherlands Journal of Geosciences – Geologie en Mijnbouw*, 94, 93–108. https://doi.org/10.1017/njg.2014.43

Bardet, N., Houssaye, A., Vincent, P., Suberbiola, X. P., Amaghzaz, M., Jourani, E., & Meslouh, S. (2015). Mosasaurids (Squamata) from the Maastrichtian phosphates of Morocco: biodiversity, palaeobiogeography and palaeoecology based on tooth morphoguilds. *Gondwana Research*, 27(3), 1068–1078.

Bastiaans, D., Kroll, J. J., Cornelissen, D., Jagt, J. W. M., & Schulp, A. S. (2020). Cranial palaeopathologies in a Late Cretaceous mosasaur from the Netherlands. *Cretaceous Research*, 112, 104425. https://doi.org/10.1016/j.cretres.2020.104425

Bell Jr., G. L. & Barnes, K. R. (2007). First record of stomach contents in *Tylosaurus nepaeolicus* and comments on predation among mosasauridae *Second Mosasaur Meeting Abstract Booklet and Field Guide, Sternberg Museum of Natural History, Hays Kansas*, pp. 9–10.

Bernard, A., Lécuyer, C., Vincent, P., Amiot, R., Bardet, N., Buffetaut, E., Cuny, G., Fourel, F., Martineau, F., Mazin, J-M., & Prieur, A. (2010). Regulation of body temperature by some Mesozoic marine reptiles. *Science*, 328(5984), 1379-1382.

Camp, C. L. (1942). California mosasaurs. *Memoirs of the University of California 13, vi + 1–67.*

Cooper, S. L., Marson, K. J., Smith, R. E., & Martill, D. (2022). Contrasting preservation in pycnodont fishes reveals first record of regurgitalites from the Upper Cretaceous (Maastrichtian) Moroccan phosphate deposits. *Cretaceous Research*, 131, 105111. https://doi.org/10.1016/j.cretres.2021.105111

Dollo, L. (1913). Globidens Fraasi, Mosasaurien Mylodonte Nouveau du Maestrichtien (Crétacé Supérieur) du Limbourg et l'éthologie de la Nutrition chez les Mosasauriens. *Archives de Biologie*, 28, 609–626.

Dollo, L. (1887). Le hainosaure et les nouveaux vertébrés fossiles du Musée de Bruxelles. *Revue des Questions Scientifiques*, 21, 504–539.

Einarsson, E., Lindgren, J., Kear, B. P., & Siverson, M. (2010). Mosasaur bite marks on a plesiosaur propodial from the Campanian (Late Cretaceous) of southern Sweden. *GFF*, 132(2), 123–128.

Everhart, M. J. (2002a). Remains of immature mosasaurs (Squamata; Mosasauridae) from the Niobrara Chalk (Late Cretaceous) argue against nearshore nurseries. *Journal of Vertebrate Paleontology*, 22 (Suppl. to 3), 52A.

Everhart, M. J. (2002b). New data on cranial measurements and body length of the mosasaur *Tylosaurus nepaeolicus* (Squamata: Mosasauridae), from the Niobrara Formation of Western Kansas. *Transactions of the Kansas Academy of Science*, 105, 33–43.

Everhart, M. J. (2004a). Plesiosaurs as the food of mosasaurs; new data on the stomach contents of a *Tylosaurus proriger* (Squamata; Mosasauridae) from the Niobrara Formation of western Kansas. *The Mosasaur*, 7, 41–46.

Everhart, M. J. (2004b). Late Cretaceous interaction between predators and prey. Evidence of feeding by two species of shark on a mosasaur. *PalArch*, 1, 1–6

Everhart, M. J. (2007). Remains of young mosasaurs from the Smoky Hill Chalk (Upper Coniacian-Lower Campanian) of western Kansas. In M. J. Everhart (Ed.), *Second Mosasaur Meeting Abstract Booklet and Field Guide* (pp. 2–6). Sternberg Museum of Natural History, Hays, Kansas.

Everhart, M. J. (2008). A bitten skull of *Tylosaurus kansasensis* (Squamata: Mosasauridae) and a review of mosasaur-on-mosasaur pathology in the fossil record. *Transactions of the Kansas Academy of Science*, 111(3), 251–262.

Fernandes, A. E., Mateus, O., Andres, B., Polcyn, M. J., Schulp, A. S., Gonçalves, A. O., & Jacobs, L. L. (2022). Pterosaurs from the Late Cretaceous of Angola. *Diversity*, 14(9), 741.

Fischer, V., Bennion, R. F., Foffa, D., MacLaren, J. A., McCurry, M. R., Melstrom, K. M., & Bardet, N. (2022). Ecological signal in the size and shape of marine amniote teeth. *Proceedings of the Royal Society B*, 289(1982), p. 20221214. https://doi.org/10.1098/rspb.2022.1214

Fisher, D. C. (1981). Crocodilian scatology, microvertebrate concentrations, and enamel-less teeth. *Paleobiology*, 7(2), 262–275.

Géczy, C. (2009). Cannibalism in captive *Varanus timorensis*. *Biawak*, 3(2), 61-63.

Harrell Jr, T. L., Pérez-Huerta, A., & Suarez, C. A. (2016). Endothermic mosasaurs? Possible thermoregulation of Late Cretaceous mosasaurs (Reptilia, Squamata) indicated by stable oxygen isotopes in fossil bioapatite in comparison with coeval marine fish and pelagic seabirds. *Palaeontology*, 59(3), 351-363.

Jacobs, L. L., Mateus, O., Polcyn, M. J., Schulp, A. S., Antunes, M. T., Morais, M.-L., & Tavares, T. da S. (2006). The occurrence and geological setting of Cretaceous dinosaurs, mosasaurs, plesiosaurs, and turtles from Angola. *Journal of the Paleontological Society of Korea*, 22(1), 91–110.

Jacobs, L. L., Polcyn, M. J., Mateus, O., Schulp, A. S., Gonçalves, A. O., & Morais, M.-L. (2016). Post-Gondwana Africa and the vertebrate history of the Angolan Atlantic coast. *Memoirs of Museum Victoria*, 74, 343–362.

Jacobs, L. L., Mateus, O., Polcyn, M. J., Schulp, A. S., Scotese, C. R., Goswami, A., Ferguson, K. M., Robbins, J. A., Vineyard, D. P., & Neto, A. B. (2009). Cretaceous paleogeography, paleoclimatology, and amniote biogeography of the low and mid-latitude South Atlantic Ocean. *Bulletin of the Geological Society of France*, 180(4), 333–341.

Jacobs, L. L., Schröder, S., da Sousa, N., Dixon, R., Fiordalisi, E., Marechal, A., Mateus, O., Nsungani, P. C., Polcyn, M. J., do Couto, G., Pereira, R., Rochelle-Bates, N., Schulp, A. S., Scotese, C. R., Sharp, I., Gaudari Silvano, C., Swart, R., & Vineyard, D. P. (in press). The Atlantic jigsaw puzzle and the geoheritage of Angola. In R. M. Clary, E. J. Pyle, & W. M. Andrews (Eds.), *Geology's Significant Sites and their Contributions to Geoheritage.* Geological Society, London, Special Publications.

Kauffman, E. G. (2004). Mosasaur predation on Upper Cretaceous nautiloids and ammonites from the United States Pacific Coast. *Palaios*, 19(1), 96–100.

King, D. R. & King, R. A. (2004). *Varanus rosenbergi*. In E. R. Pianka & D. R. King (Eds.), *Varanoid Lizards of the World* (pp. 438–450). Indiana University Press, Bloomington, Indiana.

Konishi, T., Brinkman, D., Massare, J. A., & Caldwell, M. W. (2011). New exceptional specimens of *Prognathodon overtoni* (Squamata, Mosasauridae) from the upper Campanian of Alberta, Canada, and the systematics and ecology of the genus. *Journal of Vertebrate Paleontology*, 31(5), 1026–1046.

Konishi, T., Newbrey, M. G., & Caldwell, M. W. (2014). A small, exquisitely preserved specimen of *Mosasaurus missouriensis* (Squamata, Mosasauridae) from the upper Campanian of the

Bearpaw Formation, western Canada, and the first stomach contents for the genus. *Journal of Vertebrate Paleontology*, 34(4), 802–819.

Lécuyer, C., Grandjean, P., O'Neil, J. R., Cappetta, H., & Martineau, F. (1993). Thermal excursions in the ocean at the Cretaceous—Tertiary boundary (northern Morocco): $\delta^{18}O$ record of phosphatic fish debris. *Palaeogeography, Palaeoclimatology, Palaeoecology*, 105(3-4), 235-243.

Longrich, N. R., Jalil, N. E., Khaldoune, F., Yazami, O. K., Pereda-Suberbiola, X., & Bardet, N. (2022). *Thalassotitan atrox*, a giant predatory mosasaurid (Squamata) from the upper Maastrichtian phosphates of Morocco. *Cretaceous Research*, 140, 105315.

Martin, J. E. & Bjork, P. P. (1987). Gastric residues associated with a mosasaur from the Late Cretaceous (Campanian) Pierre Shale in South Dakota. In J. E. Martin & G. E. Ostrander (Eds.), *Papers in Vertebrate Paleontology in honor of Morton Green* (pp. 68-72). Dakoterra, 3.

Martin J. E. & Fox J. E. (2007). Stomach contents of *Globidens*, a shell-crushing mosasaur (Squamata), from the late Cretaceous Pierre Shale, big bend area of the Missouri River, central South Dakota. In J. E. Martin & D. C. Parris (Eds.), *Geology and Paleontology of the Late Cretaceous Marine Deposits of the Dakotas* (pp. 167-176). Geological Society of America, Special Paper, 427.

Marx, M. P., Mateus, O., Polcyn, M. J., Schulp, A. S., Gonçalves, A. O., & Jacobs, L. L. (2021). The cranial anatomy and relationships of *Cardiocorax mukulu* (Plesiosauria: Elasmosauridae) from Bentiaba, Angola. *PLoS ONE*, 16(8), e0255773.

Massare, J. A. (1987). Tooth morphology and prey preference of Mesozoic marine reptiles. *Journal of Vertebrate Paleontology*, 7(2), 121-137.

Mateo, J. A. & Pleguezuelos, J. M. (2015). Cannibalism of an endemic island lizard (genus *Gallotia*). *Zoologischer Anzeiger-A Journal of Comparative Zoology*, 259, 131-134.

Mateus, O., Callapez, P. M., Polcyn, M. J., Schulp, A. S., Gonçalves, A.O., & Jacobs, L. L. (2019). The Fossil Record of Biodiversity in Angola Through Time: A Paleontological Perspective. In B. J. Huntley et al. (Eds.), *Biodiversity of Angola*, (pp. 53–76). https://doi.org/10.1007/978-3-030-03083-4_4

Mateus, O., Marzola, M. Schulp, A. S., Jacobs, L. L., Polcyn, M. J., Pervov, V., Goncalves, A. O., & Morais, M.-L. (2017). Angolan ichnosite in a diamond mine shows the presence of a large terrestrial mammaliamorph, a crocodylomorph, and sauropod dinosaurs in the Early Cretaceous of Africa. *Palaeogeography, Palaeoclimatology, Palaeoecology*, 471, 220–232.

Mateus, O., Jacobs, L. L., Polcyn, M. J., Schulp. A. S., Vineyard, D. P., Antunes, M. T., & Neto, A. B. (2009). The oldest African eucryptodiran turtle from the Cretaceous of Angola. *Acta Palaeontologica Polonica*, 54, 581–588.

Mateus, O., Jacobs, L. L., Schulp. A. S., Polcyn, M. J., Tavares, T. S., Neto, A. B., Morais, M. L., & Antunes, M. T. (2011). *Angolatitan adamastor*, a new sauropod dinosaur and the first record from Angola. *Anais da Academia Brasileira de Ciências*, 83(1), 221–233.

Mateus, O., Polcyn, M. J., Jacobs, L. L., Araújo, R., Schulp, A. S., Marinheiro, J., Oereira, B., & Vineyard, D. (2012). Cretaceous amniotes from Angola: Dinosaurs, pterosaurs, mosasaurs, plesiosaurs, and turtles. *V Jornadas Internacionales sobre Paleontología de Dinosaurios y su Entorno*, 75–105, Salas de los Infantes, Burgos.

McBrayer, L. D. & Reilly, S. M. (2002). Prey processing in lizards: behavioral variation in sit-and-wait and widely foraging taxa. *Canadian Journal of Zoology*, 80(5), 882–892.

Mitchell, J. C. (1986). Cannibalism in Reptiles: A Worldwide Review. *Herpetological circular No. 15. Society for the Study of Amphibians and Reptiles*, Lawrence, Kansas.

Myers, T. S., Polcyn, M. J., Mateus, O., Vineyard, D. P., Gonçalves, A. O., & Jacobs, L. L. (2017). A new durophagous stem cheloniid turtle from the Lower Paleocene of Cabinda, Angola. *Papers in Palaeontology*, 2017, 1–16.

Neumann, C. & Hampe, O. (2018). Eggs for breakfast? Analysis of a probable mosasaur biting trace on the Cretaceous echinoid *Echinocorys ovata* Leske, 1778. *Fossil Record*, 21(1), 55–66.

Polcyn, M. J., Jacobs, L. L., Schulp, A. S., & Mateus, O. (2014). Physical drivers of mosasaur evolution. *Palaeogeography, Palaeoclimatology, Palaeoecology*, 400, 17–27.

Polcyn, M. J., Jacobs, L. L., Schulp, A. S., & Mateus, O. (2010). The North African mosasaur *Globidens phosphaticus* from the Maastrichtian of Angola. *Historical Biology*, 22(1–3), 175–185.

Robbins, J. A., Ferguson, K. M., Polcyn, M. J., & Jacobs, L. L. (2008). Application of stable carbon isotope analysis to mosasaur ecology. In M. J. Everhart (Ed.), *Proceedings of the Second Mosasaur Meeting, Hays, Kansas* (pp. 123–130).

Russell, D. A. (1967). Systematics and morphology of American mosasaurs. *Peabody Museum of Natural History, Yale, Bulletin*, 23, 1–241.

Schulp, A. S., Polcyn, M. J., Mateus, O., Jacobs, L. L., Morais, M.-L., & Tavares, T. da S. (2006). New mosasaur material from the Maastrichtian of Angola, with notes on the phylogeny, distribution and paleoecology of the genus *Prognathodon*. *Publicaties van het Natuurhistorisch Genootschap in Limburg*, 45(1), 57–67.

Schulp, A. S., Polcyn, M. J., Mateus, O., Jacobs, L. L., & Morais, M.L. (2008). A new species of *Prognathodon* (Squamata, Mosasauridae) from the Maastrichtian of Angola, and the affinities of the mosasaur genus *Liodon*. In M. J. Everhart (Ed.), *Proceedings of the Second Mosasaur Meeting, Hays, Kansas* (pp. 1–12).

Schulp, A. S., Polcyn, M. J., Mateus, O., & Jacobs, L. L. (2013). Two rare mosasaurs from the Maastrichtian of Angola and the Netherlands. *Netherlands Journal of Geosciences*, 92(1), 3–10.

Shine, R., Harlow, P. S., & Keogh, J. S. (1996). Commercial harvesting of giant lizards: the biology of water monitors *Varanus salvator* in southern Sumatra. *Biological Conservation*, 77(2-3), 125−134.

Sternberg, C. H. (1922). Explorations of the Permian of Texas and the chalk of Kansas, 1918. *Kansas Academy of Science, Transactions*, 30/1, 119–120.

Srichairat, N., Taksintum, W., & Chumnanpuen, P. (2018). Gross morphological structure of digestive system in water monitor lizard *Varanus salvator* (Squamata: Varanidae). *Walailak Journal of Science and Technology (WJST)*, 15(3), 245–253.

Stanner, M. (2004). *Varanus griseus*. In E. R. Panaka & D. R. King (Eds.), *Varanoid Lizards of the World* (pp. 104−132). Indiana University Press, Bloomington, Indiana.

Strganac, C., Salminen, J., Jacobs, L. L., Polcyn, M. J., Ferguson, K. M., Mateus, O., Schulp, A. S., Morais, M.-L., Tavares, T. da S., & Gonçalves, A. O. (2014). Carbon isotope stratigraphy, magneto-stratigraphy, and $^{40}Ar/^{39}Ar$ age of the Cretaceous South Atlantic coast, Namibe Basin, Angola. *Journal of African Earth Sciences*, 9, 452–462. https://doi.org/10.1016/j.jafrearsci.2014.03.003

Strganac, C., Jacobs, L. L., Polcyn, M. J., Ferguson, K. M., Mateus, O., Gonçalves, A. O., Morais, M.-L., & Tavares, T. da S. (2015a). Geological setting and paleoecology of the Upper Cretaceous Bench 19 marine vertebrate bonebed at Bentiaba, Angola. *Netherlands*

Journal of Geosciences – Geologie en Mijnbouw, 96(1), 29–33. https://doi.org/10.1017/njg.2014.32

Strganac, C., Jacobs, L. L., Polcyn, M. J., Ferguson, K. M., Mateus, O., Gonçalves, A. O., Morais, M.-L., & Tavares, T. da S. (2015b). Stable oxygen isotope chemostratigraphy and paleotemperature regime of mosasaurs at Bentiaba, Angola. *Netherlands Journal of Geosciences – Geologie en Mijnbouw,* https://doi.org/10.1017/njg.2015.1

Strong, C. R., Caldwell, M. W., Konishi, T., & Palci, A. (2020). A new species of longirostrine plioplatecarpine mosasaur (Squamata: Mosasauridae) from the Late Cretaceous of Morocco, with a re-evaluation of the problematic taxon *'Platecarpus' ptychodon*. *Journal of Systematic Palaeontology*, 18(21), 1769–1804.

Street, H. P. & Caldwell, M. W. (2017). Rediagnosis and redescription of *Mosasaurus hoffmannii* (Squamata: Mosasauridae) and an assessment of species assigned to the genus *Mosasaurus*. *Geological Magazine*, 154(3), 521–557.

Schwenk, K. (2000b). Feeding in lepidosaurs. In K. Schwenk (Ed.), *Feeding* (pp. 175−291). Academic Press, New York.

Tykoski, R. S. & Polcyn, M. J. (2023). "Tis but a scratch!" Said the Black Knight; Severe Craniofacial Pathologies in a *Tylosaurus* from the Ozan Formation (Campanian) of Northeast Texas. *Journal of Vertebrate Paleontology, Program and Abstracts*, 2023, 428L.

Wang, X., Miao, D., & Zhang, Y. (2005). Cannibalism in a semi-aquatic reptile from the Early Cretaceous of China. *Chinese Science Bulletin*, 50, 281−283.

Williston, S. W. (1899). Some additional characters of mosasaurs. *Kansas University Quarterly*, 8, 39–41.

Zietlow, A. R., Boyd, C. A., & Van Vranken, N. E. (2023). A new mosasaurine from the Pierre Formation (Pembina Member: Campanian) of North Dakota. *Bulletin of the American Museum, New York, New York*, 464, 1−82.